

Space: Science & Technology
Maximum Allowable Current Determination of RBS By Using a Directed Graph Model and Greedy Algorithm
--Manuscript Draft--

Manuscript Number:	SPACE-D-23-00082R1
Full Title:	Maximum Allowable Current Determination of RBS By Using a Directed Graph Model and Greedy Algorithm
Short Title:	
Article Type:	Research Article
Section/Category:	Space Technology
Keywords:	Reconfigurable Battery System; Maximum Allowable Current; Directed Graph Model; Greedy Algorithm
Corresponding Author:	Cheng Qian CHINA
Corresponding Author Secondary Information:	
Corresponding Author's Institution:	
Order of Authors:	Binghui Xu Guangbin Hua Cheng Qian Quan Xia Bo Sun Yi Ren Zili Wang
Order of Authors Secondary Information:	
Manuscript Region of Origin:	CHINA
Abstract:	Reconfigurable battery systems (RBSs) present a promising alternative to traditional battery systems due to their flexible and dynamically changeable topological structure that can be adapted to different battery charging and discharging strategies. During RBS operation, a critical system parameter known as the maximum allowable current (MAC) become pivotal. This parameter is instrumental in maintaining the current of each individual battery within a safe range and serves as a guiding indicator for the system's reconfiguration, thereby ensuring its safety and reliability. This paper proposes a method to calculate the MAC of arbitrary RBSs using a greedy algorithm in conjunction with a directed graph model. By introducing the shortest path of the battery, the greedy algorithm transforms the enumeration of switch states in the brute-force algorithm into the combination of the shortest paths, which greatly increases the efficiency with which the MAC is determined. The directed graph model, based on the equivalent circuit, provides a specific method for calculating the MAC of a given structure. The proposed method is validated on two published four-battery-RBSs and one with a more complex structure. The results are the same as those of the brute-force algorithm, but the proposed method significantly improves the computational efficiency ($N_s 2^{[N_s - N_b]} \log_{10} N_b$ times faster than the brute force algorithm for an RBS with N_b batteries and N_s switches, theoretically). The main advantage of the proposed method is its ability to calculate the MAC of RBSs with arbitrary structures, even in scenarios with random isolated batteries.
Suggested Reviewers:	
Opposed Reviewers:	

Additional Information:	
Question	Response
<p>Authorship As corresponding author, I confirm that all authors have:</p> <ul style="list-style-type: none"> • Seen and approved the submitted manuscript and all related materials. • Agreed to be listed as an author and agreed to the submitted order of authorship. <p>(We will verify this requirement with all co-authors upon submission. Non-compliance may lead to rejection.)</p>	Yes

Dear Dr. Tian and the anonymous reviewer,

On behalf of my co-authors, we thank you very much for giving us an opportunity to revise our manuscript, we appreciate editor and reviewer very much for their positive and constructive comments and suggestions on our manuscript entitled “Maximum Allowable Current Determination of RBS By Using a Directed Graph Model and Greedy Algorithm”(ID:SPACE-D-23-00082).

We have studied reviewer's comments carefully and have made revision which marked in red in the paper. We have tried our best to revise our manuscript according to the comments. Specially, this manuscript has been retouched by the professional organization, to further improve the readability. Attached please find the revised version, which we would like to submit for your kind consideration.

We would like to express our great appreciation to you and reviewers for comments on our paper. Looking forward to hearing from you.

Thank you and best regards.

Dr. Cheng Qian, on behalf of all authors

Beihang University

2023.9.20

Authors' Response to Reviewer 1

Comment 1:

The authors should explain the most important achievements of the proposed method quantitatively, in the abstract.

Response:

Thanks for the reviewer's valuable feedback. We have carefully considered this suggestion and made the following modifications to address the reviewer's concern:

By introducing the shortest path (SP) of the battery, the greedy algorithm transforms the enumeration of switch states in the brute force algorithm into the combination of the SPs, resulting in more efficient computation of the maximum allowable current (MAC). We have also provided a theoretical estimation of the improvement, which is proportional to $2^{N_s - N_b} N_s \log_{10} N_b$ for an RBS with N_b batteries and N_s switches.

Here is the specific content we added in the abstract:

This paper proposes a method to calculate the MAC of arbitrary RBSs using a greedy algorithm in conjunction with a directed graph model of the RBS. By introducing the shortest path of the battery, the greedy algorithm transforms the enumeration of switch states in the brute-force algorithm into the combination of the shortest paths, which greatly increases the efficiency with which the MAC is determined. The directed graph model, based on the equivalent circuit, provides a specific method for calculating the MAC of a given structure. The proposed method is validated on two published four-battery-RBSs and one with a more complex structure. The results are the same as those of the brute-force algorithm, but the proposed method significantly improves the computational efficiency ($N_s 2^{N_s - N_b} \log_{10} N_b$ times faster than the brute force algorithm for an RBS with N_b batteries and N_s switches, theoretically). The main advantage of the proposed method is its ability to calculate the MAC of RBSs with arbitrary structures, even in scenarios with random isolated batteries.

We hope the above content provide a more quantitative explanation of the achievements of our proposed method in the abstract.

Comment 2:

The literature review in the introduction section is very short, and the related works, especially the works published in recent years, have not been well reviewed and compared, and the conclusions about the existing research gaps have not been presented.

Response:

Considering the Reviewer's suggestion, we have expanded the literature review in the introduction section to provide a comprehensive overview of the existing RBS structures (cited as [12, 13, 14, 11, 15, 16, 17] in revised manuscript) and related works on structure analyses (cited as [18, 19] in revised manuscript). Although many RBS structures have been proposed for different purposes, such as dynamically adjusting the output voltage , increasing energy utilization efficiency, and improving the system's ability to recover from battery failures, these structures also bring challenges in design and control of the systems. Therefore, several works on structure analyses, like the maximum switch current and the short-circuit problem, have been proposed to tackle these challenges recently. However, determining the MAC of RBSs remains blank according to our literature review. A straightforward method is to enumerate all possible switch states. But this method has exponentially increasing computational complexity with the number of switches, and is too ineffectual to apply.

Here is the specific modification we made in the introduction:

Recently, various types of RBSs with different flexibility and reconfigurability have been designed to meet application requirements. For example, Ci et al. [12] proposed an RBS structure that dynamically adjusts the battery discharge rate

to fully exploit the available capacity of each battery.Jan's [13, 14] structures reconfigure structures with variant batteries in series to reach the (constantly changing) voltage requirements during electric vehicle charging.As shown in Fig. 1a, the structure proposed by Visairo et al. [11] changes the system's output voltage based on the load conditions, thereby reducing the power loss of the voltage regulator during the power supply process and improving the efficiency of energy use.Also, to enhance the energy efficiency of the system, Lawson et al. [15] and He et al. [16] proposed simplified structures that have fewer switches than Visairo's design.Kim et al. [17] improved the system's ability to recover from battery failures by introducing multiple ports into the structure.The complex structure between batteries and switches gives RBSs flexibility but also creates challenges in the design and control of the system.Thus, several approaches to analyze the RBS structure and performance have been proposed to tackle these challenges.For instance,Han et al. [18] derived an analytical expression for the maximum switch current during battery system reconfiguration for a specific RBS structure.This helps guide the selection of switches and supports the design of RBS hardware.Chen et al. [19] proposed a systematic approach based on sneak circuit theory to fundamentally avoid the short-circuit problem of RBSs:They thoroughly analyzed all paths between the cathode and anode of each battery in the RBS and identified paths that only contain switches as short-circuit paths for pre-checking before system reconfiguration.In spite of the maximum switch current mentioned above, the maximum allowable current (MAC), defined as the maximum allowed current under the constraints of the battery cell, is another critical indicator of RBSs that needs to be evaluated during the design or control of the system.The MAC helps the designers assess whether the RBS meets the output current requirements and contributes to the formulation of appropriate and safe management strategies for the battery management system.Unfortunately, few studies have analyzed the RBS structure to determine the RBS MAC.An intuitive

and straightforward method is to enumerate all possible switch states and calculate the output current of the system under each reconfigured structure. However, this method is inefficient and time-consuming, especially for RBSs with a large number of switches.

Thanks again for the reviewer's comments, which have greatly improved the quality and comprehensiveness of our manuscript.

Comment 3:

It is necessary for the authors to clearly state research contribution and achievements as bullet points at the end of the Introduction section.

Response:

We appreciate and accept your suggestion and have added a clear statement of the contributions in the second-to-last paragraph of the Introduction, as shown below:

The main contributions of this paper can be summarized as follows:

- An efficient method is proposed to determine the MAC of RBSs with arbitrary structures, including scenarios with isolated batteries.
- A greedy algorithm is applied to solve the MAC problem, the computational complexity of which is greatly reduced compared with the brute-force algorithm.
- An improved directed graph model is introduced to provide a specific method for calculating the MAC of a given structure.

Comment 4:

The authors need to present the complexity of their proposed method and compare it with some other state-of-the-art or successful classic methods.

Response:

We totally agree with the reviewer's suggestion. It is indeed necessary to analyze the complexity of the proposed method and compare it with other existing methods.

We have derived the average time complexity of our proposed greedy algorithm-based MAC determination method to be approximately $O(2^{N_b} N_s^2 \log_{10} N_b)$, where N_b and N_s are the number of batteries and switches, respectively. However, as mentioned in our response to Comment 2, there is a blank in the literature regarding MAC determination methods. The brute force method, the most straightforward and intuitive method, is used as a benchmark for comparison, the time complexity of which is $O(2^{N_s} N_s^3)$. Since the number of switches in RBS is typically 3 to 5 times the batteries, the method we proposed is theoretically more efficient than the brute force method. It has been validated by the case study in the manuscript.

The detailed derivation and discussion of the above points have been added to the revised manuscript under the Discussion subsection. Here is the specific content:

The literature contains no report on an algorithm for calculating the MAC of an RBS. The brute-force algorithm, which goes through all possible switch states, is the most straightforward way to determine the MAC and is used as a benchmark for the proposed greedy algorithm. If an RBS has N_b batteries and N_s switches and the corresponding directed graph has N nodes, 2^{N_s} iterations are required to traverse all reconfigured structures. Calculating each reconfigured structure using Eqs. (7)–(10) requires matrix inversion and matrix multiplication, which has a time complexity of $O(N^3 + 2N^2 N_b + N^2 N_s + NN_b^2)$. Therefore, the time complexity of the brute-force algorithm is $O((N^3 + 2N^2 N_b + N^2 N_s + NN_b^2)2^{N_s})$. The greedy algorithm proposed in this paper requires that SP be found for each battery, which

requires N_b iterations. Each SP can be obtained by several applications of Dijkstra's algorithms. Therefore, the total time complexity for calculating all SPs is $O(N_b(N_b + 2N_s) \log_{10} N)$. According to Appendix 1, the RBS can reconfigure $C_{N_b}^{N_{\text{set}}}$ structures by selecting N_{set} batteries from N_b batteries, which gives $\sum_{N_{\text{set}}=1}^{N_b} C_{N_b}^{N_{\text{set}}} / N_b \approx 2^{N_b} N_b^{-1}$ on average. Thus, with the bisection method, the time complexity of the greedy algorithm is $O((N^3 + 2N^2 N_b + N^2 N_s + NN_b^2) 2^{N_b} N_b^{-1} \log_{10} N_b + N_b(N_b + 2N_s) \log_{10} N)$. Based on currently proposed RBS structures [23, 24, 25, 26, 27, 28], the number N_b of batteries, N_s of switches, and N of nodes are quantitatively related as follows: $N_s \approx (3-5)N_b$, $N \approx N_s$. After simplifying, the time complexity of the method with greedy algorithm is $O(2^{N_b} N_s^2 \log_{10} N_b)$, while it is $O(2^{N_s} N_s^3)$ for the method with brute force algorithm. Therefore, as the RBS grows, especially in the number of switches, the greedy algorithm gains an advantage over the brute-force algorithm. This is confirmed by the number of structures required to determine the MAC in the previous section. Compared with the brute-force algorithm, the method based on the greedy algorithm is 3 000 to 48 000 times more efficient, which is theoretically $N_s 2^{N_s - N_b} \log_{10} N_b$ times according to the above time-complexity analysis. This benefits from two key points:

- (1) The SPs guide the RBS to reconfigure reasonable structures rather than blindly going through all possible structures. This reduces the complexity from 2^{N_s} to 2^{N_b} , which is the main reason for the improvement in efficiency.
- (2) The bisection method further accelerates this process, reducing the complexity from 2^{N_b} to $2^{N_b} N_B^{-1} \log_{10} N_b$.

Comment 5:

The authors don't discuss the limitations of the study correctly.

Response:

We are sorry for our negligence of the limitations of the study. As far as we are concerned, although the method we proposed is strongly efficient than the brute force method, it still has a exponential relationship with the number of batteries. That means unsufferable time will be costed for systems with large number of batteries.

Here is the specific content we added in the discussion:

However, the greedy algorithm proposed in this paper still contains exponential terms in the time complexity, which means it may not be able to handle extremely large RBS structures having large N_b .

Comment 6:

Some typos should be double check.

Response:

We are very sorry for our incorrect writing, and have carefully checked the manuscript and corrected the typos.

Comment 7:

The author should explain more why solution quality of their proposed approach is much better than the others?

Response:

We appreciate the reviewer's concern regarding the explanation of why the solution quality of our proposed approach is better to others. However, after careful literature research, we would like to clarify that there are currently no existing works on the MAC

determination of RBSs that we could compare our solution with. Therefore, it is not possible to directly compare the solution quality of our proposed approach with others.

Comment 8:

Authors should mention some novel works in the field in the introduction, specially refer to this 2023 reference: An efficient lightweight algorithm for scheduling tasks onto dynamically reconfigurable hardware using graph-oriented simulated annealing, which uses graph-based method. Mention and refer to it in the introduction section.

Response:

Thanks to the reviewer's suggestion, we have introduced two novel works in the RBS structure analysis field in the introduction, which respectively study the maximum switch current and the short-circuit problem. Here is the specific content we added in the introduction:

The complex structure between batteries and switches gives RBSs flexibility but also creates challenges in the design and control of the system. Thus, several approaches to analyze the RBS structure and performance have been proposed to tackle these challenges. For instance, Han et al. [18] derived an analytical expression for the maximum switch current during battery system reconfiguration for a specific RBS structure. This helps guide the selection of switches and supports the design of RBS hardware. Chen et al. [19] proposed a systematic approach based on sneak circuit theory to fundamentally avoid the short-circuit problem of RBSs. They thoroughly analyzed all paths between the cathode and anode of each battery in the RBS and identified paths that only contain switches as short-circuit paths for pre-checking before system reconfiguration.

The reviewer also mentioned the work "An efficient lightweight algorithm for scheduling tasks onto dynamically reconfigurable hardware using graph-oriented simulated

annealing”, sepcially. After carefully reading and fully discussion, we reached a conclusion that this paper is not relevant to our research. Although this paper uses a graph-based method, whose name is similar to the method described in our paper, it mainly studies the task scheduling problem in time series. While our research is about the maximum allowable current of RBS structure, which belongs to the field of structure analysis. Therefore, we think it is not appropriate to include this paper in our introduction and will not cite it.

Comment 9:

Authors need to explain about the accuracy, sufficiency and reliability of their results? How do they verify and validate the results?

Response:

Thanks for the reviewer’s valuable feedback. We have carefully considered the reviewer’s question. In response, we complemented the computation and validation with the brute force method and provided more detailed explanation and discussion.

In the Case study section of the paper, we investigated three RBS structures, two of which are from published literatures (see references [15, 11] in revised manuscript) and the other is designed by ourselves, as shown in Figs. 1a, 1b, and 1c, respectively. The results of the three RBS structures calculated by our proposed method are shown in Tabs. 1, 2, and 3, respectively. The results by brute force method are shown in Tabs. 4, 5, and 6, respectively.

On the one hand, as shown in the Tabs. 1 – 6, the reconfigured structure results from greedy algorithm are consistent with the results from the brute force algorithm. Since the brute force algorithm enumerates all possible reconfigured structures, it ensures that we obtain the global optimal solution. On the other hand, the output current of the system calculated by our directed graph model is consistent with the experience and common sense. To illustrate this, the RBS in Fig. 1c is taken as an example here. The

four batteries in this system can be divided into two groups: group g_A has B_1 and B_2 ; group g_B has B_3 and B_4 . The relationship between the two batteries in each group can be switched between series and parallel by reconfiguring the structure. While the two groups can only connect in series or disconnect. Therefore, this system's MAC is the maximum of the MAC of the two groups (i.e., $\max[\text{MAC}(g_A), \text{MAC}(g_B)]$). Both g_A and g_B are the two-battery and degenerated structure of the RBS in Fig. 1b, and have the same MAC (i.e., 2). Therefore, the MAC of the RBS in Fig. 1c is 2, consistent with the result shown in Tab. 3.

We hope the above content can address the reviewer's concerns. The above content corresponds to lines 276 to 283, and lines 289 to 294 of our revised manuscript without changes marked.

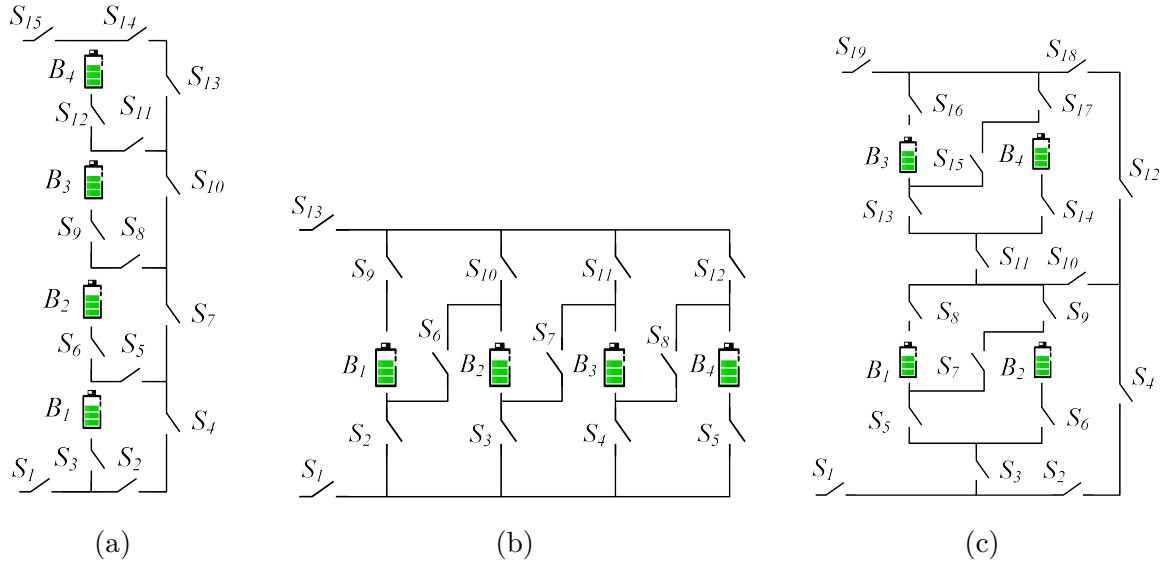


Figure 1: The four-battery RBS structures proposed by (a)Lawson[15], (b)Visairo[11] and (c)this paper.

Table 1: MAC Calculating result of the RBS structure in Figure 1a with our method.

Structure	Figure 1a with 4 batteries and 15 switches
Switch ON	$S_1, S_3, S_5, S_7, S_{10}, S_{13}, S_{14}, S_{15}$
I_o	$u_b/(R_o + r_b)$
\mathbf{I}_b	$[u_b/(R_o + r_b), 0, 0, 0]$
$\max \eta$	1
computed structure count	11

Table 2: MAC Calculating result of the RBS structure in Figure 1b with our method.

Structure	Figure 1b with 4 batteries and 13 switches
Switch ON	$S_1, S_2, S_3, S_4, S_5, S_9, S_{10}, S_{11}, S_{12}, S_{13}$
I_o	$4u_b/(4R_o + r_b)$
\mathbf{I}_b	$[u_b/(4R_o + r_b), u_b/(4R_o + r_b), u_b/(4R_o + r_b), u_b/(4R_o + r_b)]$
$\max \eta$	4
computed structure count	1

Table 3: MAC Calculating result of the RBS structure in Figure 1c with our method.

Structure	Figure 1c with 4 batteries and 19 switches
Switch ON	$S_1, S_3, S_5, S_6, S_8, S_9, S_{10}, S_{12}, S_{18}, S_{19}$
I_o	$2u_b/(2R_o + r_b)$
\mathbf{I}_b	$[u_b/(2R_o + r_b), u_b/(2R_o + r_b), 0, 0]$
$\max \eta$	2
computed structure count	11

Table 4: MAC Calculating result of the RBS structure in Figure 1a with brute force method.

Structure	Figure 1a with 4 batteries and 15 switches
Switch ON	$S_1, S_3, S_5, S_7, S_{10}, S_{13}, S_{14}, S_{15}$
I_o	$u_b/(R_o + r_b)$
\mathbf{I}_b	$[u_b/(R_o + r_b), 0, 0, 0]$
$\max \eta$	1
computed structure count	32768

Table 5: MAC Calculating result of the RBS structure in Figure 1b with brute force method.

Structure	Figure 1b with 4 batteries and 13 switches
Switch ON	$S_1, S_2, S_3, S_4, S_5, S_9, S_{10}, S_{11}, S_{12}, S_{13}$
I_o	$4u_b/(4R_o + r_b)$
\mathbf{I}_b	$[u_b/(4R_o + r_b), u_b/(4R_o + r_b), u_b/(4R_o + r_b), u_b/(4R_o + r_b)]$
$\max \eta$	4
computed structure count	8192

Table 6: MAC Calculating result of the RBS structure in Figure 1c with brute force method.

Structure	Figure 1c with 4 batteries and 19 switches
Switch ON	$S_1, S_3, S_5, S_6, S_8, S_9, S_{10}, S_{12}, S_{18}, S_{19}$
I_o	$2u_b/(2R_o + r_b)$
\mathbf{I}_b	$[u_b/(2R_o + r_b), u_b/(2R_o + r_b), 0, 0]$
$\max \eta$	2
computed structure count	524288

¹ Maximum Allowable Current Determination of RBS By Using
² a Directed Graph Model and Greedy Algorithm

³ Binghui Xu^{1†}, Guangbin Hua^{1†}, Cheng Qian^{1*}, Quan Xia^{1,2}, Bo Sun¹, Yi Ren¹, and
⁴ Zili Wang¹

⁵ ¹School of Reliability and Systems Engineering, Beihang University, Beijing, 100191,
⁶ China

⁷ ²School of Aeronautic Science and Engineering at Beihang University, Beijing, China

⁸ *Address correspondence to: cqian@buaa.edu.cn

⁹ [†]These authors contributed equally to this work.

Abstract

Reconfigurable ~~Battery Systems~~-battery systems (RBSs) present a promising alternative to traditional battery systems due to their flexible and dynamically changeable topological structure ~~subjected to that can be adapted to different~~ battery charging and discharging strategies. During ~~the operation of the RBS~~, the Maximum Allowable Current ~~RBS~~ operation, a critical system parameter known as the maximum allowable current (MAC) ~~of system that ensures each battery's current remains~~ become pivotal. This parameter is instrumental in maintaining the current of each individual battery within a safe range, ~~is a critical indicator to guide the system's reconfiguring control, and serves as a guiding indicator for the system's reconfiguration, thereby ensuring its safety and reliability. In this paper, we firstly propose a calculation method for This paper proposes a method to calculate the MAC of arbitrary RBS-RBSs~~ using a greedy algorithm in conjunction with a directed graph model of the RBS. ~~In this method, a new directed graph model is developed to model the structure of RBS, and a greedy algorithm is designed to find the possible circuit that enable MAC. Then, the MAC is calculated By introducing the shortest path of the battery, the greedy algorithm transforms the enumeration of switch states in the brute-force algorithm into the combination of the shortest paths, which greatly increases the efficiency with which the MAC is determined. The directed graph model, based on the circuit in cooperate with the equivalent model of batteries and switches. The effectiveness of the equivalent circuit, provides a specific method for calculating the MAC of a given structure. The proposed method is validated by a novel and complex RBS on two published four-battery-RBSs and one with a more complex structure. The results show that this method is capable to calculate are the same as those of the brute-force algorithm, but the proposed method significantly improves the computational efficiency ($N_s 2^{N_s - N_b} \log_{10} N_b$ times faster than the brute force algorithm for an RBS with N_b batteries and N_s switches, theoretically). The main advantage of the proposed method is its ability to calculate the~~

35 MAC of RBSs with different structures or different battery sizes efficiently, which proves the
36 correctness of this method and its potential in facilitating next-generation RBS designs and
37 applications, including battery isolation, arbitrary structures, even in scenarios with random
38 isolated batteries.

39 1 Introduction

40 Battery Energy Storage Systems energy storage systems (BESSs) are extensively employed used in
41 various applications [1], such as wind power plants [2] and space power systems [3, 4], to store and
42 release high-quality electrical energy [2, 1, 5, 4, 3][5]. Typically, a BESS consists of numerous bat-
43 teries interconnected by series-parallel circuitry to provide the required capacity storage. However,
44 traditional BESSs, in which the batteries are connected in a fixed topology, exhibit suffer from a
45 significant weakness in their worst battery due to the so-called cask effect. Moreover, if this the
46 worst battery fails during operation, it can is highly likely to exacerbate the degradation of other
47 batteries with a high possibility the other batteries, leading to reliability and safety issues [6, 7, 8].
48 These problems have become significant technical barriers in the development of many engineering
49 projects requiring high reliability, such as developing new-generation space vehicles and urgently
50 need to be addressed [9].

51 Reconfigurable Battery System (RBS) battery systems (RBSs), which can dynamically switch as
52 required to different circuit topology configurations as required, is topologies, are expected to solve
53 the above problems this problem [10]. The ability of switching circuit helps to isolate unhealthy
54 batteries, and thereby improve thereby improving the safety and reliability of the battery system.
55 Figure 1a shows To illustrate the working principle of an RBS, we consider a typical RBS structure
56 developed by Visairo [11] for dynamically adjusting the output voltage and current (Fig. 1a), which
57 is taken as an example to show the reconfiguration process. In this structure, the batteries can be
58 connected not only in series when the switches $S_1, S_5, S_6, S_7, S_8, S_9$, and S_{13} are closed (Figure
59 1b), see Fig. 1b) but also in parallel when $S_1, S_2, S_3, S_4, S_5, S_9, S_{10}, S_{11}, S_{12}$, and S_{13} are closed
60 (Figure Fig. 1c). Furthermore, when an unhealthy battery, for instance, the orange one B_3 in Figure
61 Fig. 1d, appears in the RBS, it can be isolated by opening its two adjacent switches (i.e., S_4 and
62 S_{11}), ensuring the system still remains that the system remains in a reliable working mode.

63 The complex connection Recently, various types of RBSs with different flexibility and reconfigurability
64 have been designed to meet application requirements. For example, Ci et al. [12] proposed an RBS
65 structure that dynamically adjusts the battery discharge rate to fully exploit the available capacity
66 of each battery. Jan's [13, 14] structures reconfigure structures with variant batteries in series to
67 reach the (constantly changing) voltage requirements during electric vehicle charging. As shown in
68 Fig. 1a, the structure proposed by Visairo et al. [11] changes the system's output voltage based
69 on the load conditions, thereby reducing the power loss of the voltage regulator during the power
70 supply process and improving the efficiency of energy use. Also, to enhance the energy efficiency
71 of the system, Lawson et al. [15] and He et al. [16] proposed simplified structures that have fewer
72 switches than Visairo's design. Kim et al. [17] improved the system's ability to recover from battery
73 failures by introducing multiple ports into the structure.

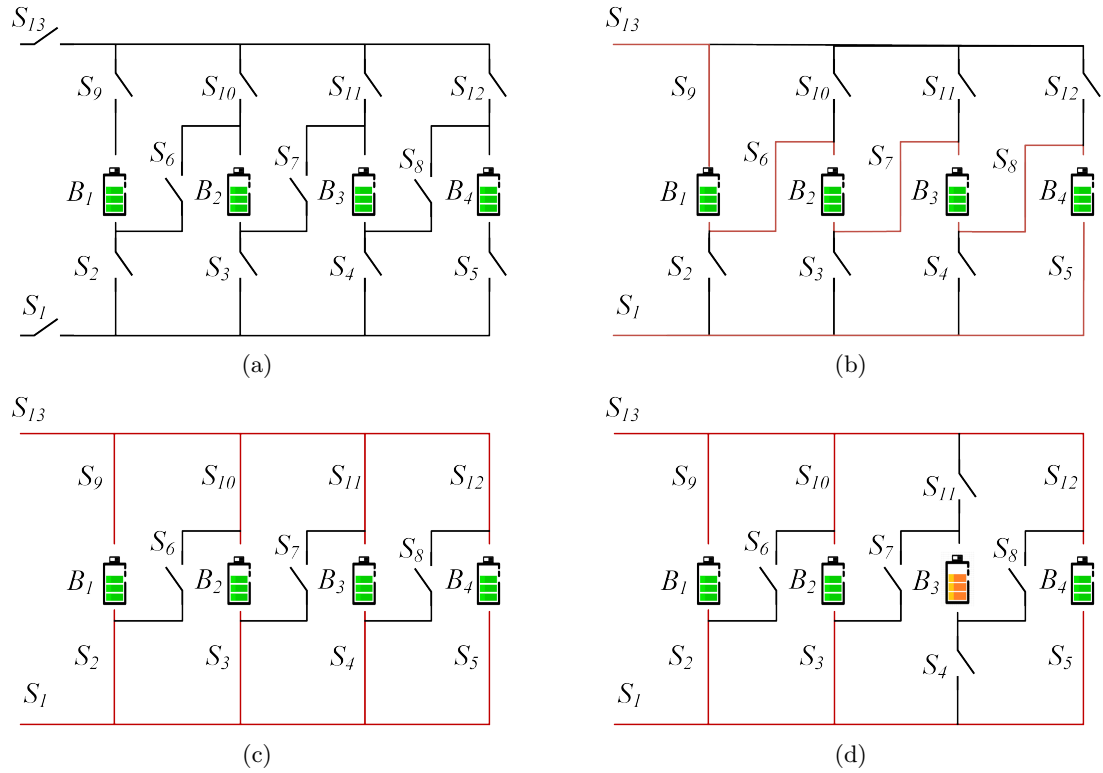


Figure 1: (a) The RBS structure proposed by Visairo[11], with all batteries in (b) series connection, (c) parallel connection, and (d) battery B_3 isolated.

74 The complex structure between batteries and switches in the RBS provides flexibility
75 but also introduces challenges in design and operational control. Unlike traditional BESSs with fixed
76 outputs, the RBS output must be dynamically adjusted by controlling switch states to meet external
77 load requirements. This necessitates additional, time-consuming output performance analysis during
78 design and corresponding control strategies. An incorrect switch control strategy may cause battery
79 short-circuiting or overload, risking the entire system. The Maximum Allowable Current creates
80 challenges in the design and control of the system. Thus, several approaches to analyze the RBS
81 structure and performance have been proposed to tackle these challenges. For instance, Han et
82 al. [18] derived an analytical expression for the maximum switch current during battery system
83 reconfiguration for a specific RBS structure. This helps guide the selection of switches and supports
84 the design of RBS hardware. Chen et al. [19] proposed a systematic approach based on sneak
85 circuit theory to fundamentally avoid the short-circuit problem of RBSs: They thoroughly analyzed
86 all paths between the cathode and anode of each battery in the RBS and identified paths that only
87 contain switches as short-circuit paths for pre-checking before system reconfiguration.

88 In spite of the maximum switch current mentioned above, the maximum allowable current
89 (MAC), an RBS performance indicator, can guide designers in addressing this issue. MAC is de-
90 fined as the maximum RBS output current that ensures each battery's current remains within a safe
91 range. Therefore, it provides a benchmark for RBS output current, protecting individual batteries
92 and identifying overall system output limits during operation. Despite its importance, no method
93 currently exists for automatically evaluating MAC for RBSs. In particular, when one or more random
94 cells are isolated, there is still no method to determine the MAC of the remaining RBS in time to
95 assist the system in adjusting the control strategy timely. A universal and automatical method for
96 calculating RBS MAC is urgently needed for practical applications. In this study, a directed graph
97 model and greedy algorithm are employed to determine the MAC of RBS and the corresponding
98 control strategy, effectively calculating the MAC for allowed current under the constraints of the
99 battery cell, is another critical indicator of RBSs that needs to be evaluated during the design or
100 control of the system. The MAC helps the designers assess whether the RBS meets the output current
101 requirements and contributes to the formulation of appropriate and safe management strategies for
102 the battery management system. Unfortunately, few studies have analyzed the RBS structure to
103 determine the RBS MAC. An intuitive and straightforward method is to enumerate all possible
104 switch states and calculate the output current of the system under each reconfigured structure.
105 However, this method is inefficient and time-consuming, especially for RBSs with a large number of
106 switches.

107 To solve this issue, this paper proposes an efficient method to evaluate the MAC of RBSs. In
108 this method, a greedy algorithm is designed to efficiently search the possible circuit topology of
109 RBSs with MAC. This algorithm transforms the enumeration of switch states in the brute-force
110 algorithm into the combination of the batteries' shortest paths. An improved direct graph model
111 that considers the voltage, the internal resistance, the MAC of the battery, and the external load
112 is also introduced to analyze the current of the RBS. The main contributions of this paper can be
113 summarized as follows:

- 114 • An efficient method is proposed to determine the MAC of RBSs with arbitrary structures,

115 including scenarios with isolated batteries.

- 116 • A greedy algorithm is applied to solve the MAC problem, the computational complexity of
117 which is greatly reduced compared with the brute-force algorithm.
- 118 • An improved directed graph model is introduced to provide a specific method for calculating
119 the MAC of a given structure.

120 The remainder of this paper is organized as follows: Section II presents the framework and details
121 of the proposed directed graph model and the greedy algorithm. Section III demonstrated discusses
122 a case study of using that uses the proposed method to determine the MAC of a novel and MACs of
123 two published four-battery RBSs and one with a more complex structure. The calculation results,
124 the algorithm's computational complexity, and scenarios such as batteries isolation also are battery
125 random isolation are also discussed. Finally, the concluding remarks are drawn presented in Section
126 IV.

127 2 Methodology

128 The central principle of this method is to make connect the batteries in RBS connected in parallel as
129 much as an RBS in parallel to the extent possible, thereby maximizing the output current of the RBS.
130 To achieve this universally and automatically achieve this, the overall process is divided into four
131 steps, as shown in Figure 2. Firstly the four steps shown in Fig. 2. First, a directed graph model
132 is established for subsequent computing, which computations. The model not only contains the
133 connected relationships between batteries and switches, but also retains the performance parameters
134 of the batteries. Subsequently, based on the equivalent circuit, the MAC problem is transformed into
135 specific objective functions and constraints. Then, the The shortest paths (SPs, where additional
136 batteries and switches on the path are penalized as distance) for the batteries are obtained then
137 obtained by using the Dijkstra algorithm to guide connect the batteries in the RBS connect in
138 parallel. Finally, a greedy algorithm is employed used to organize the switches, allowing the batteries
139 to connect via their SPs while satisfying the constraints, resulting in the MAC of the RBS.

140 2.1 Directed graph Modelmodel

141 He et al. [20] once proposed an abstracted directed graph model for an RBS, where the nodes
142 represented represent the batteries, the edges represented represent the configuration flexibility, and
143 the weight of each vertex corresponded corresponds to the battery voltage (Figure Fig. 3a). The
144 model effectively captured captures all potential system configurations and offered offers a direct
145 metric for configuration flexibility, but it did does not specify the physical implementation of the
146 connectivity between batteries, meaning that one graph might have had correspond to multiple
147 RBS structures. We previously proposed a novel directed graph model that, in contrast to differs
148 completely from He's model, used by using nodes to represent the connections between batteries
149 and switches, and directed edges to represent batteries and switches (Figure Fig. 3b), allowing for
150 a one-to-one correspondence between the RBS structure and the directed graph model. This model

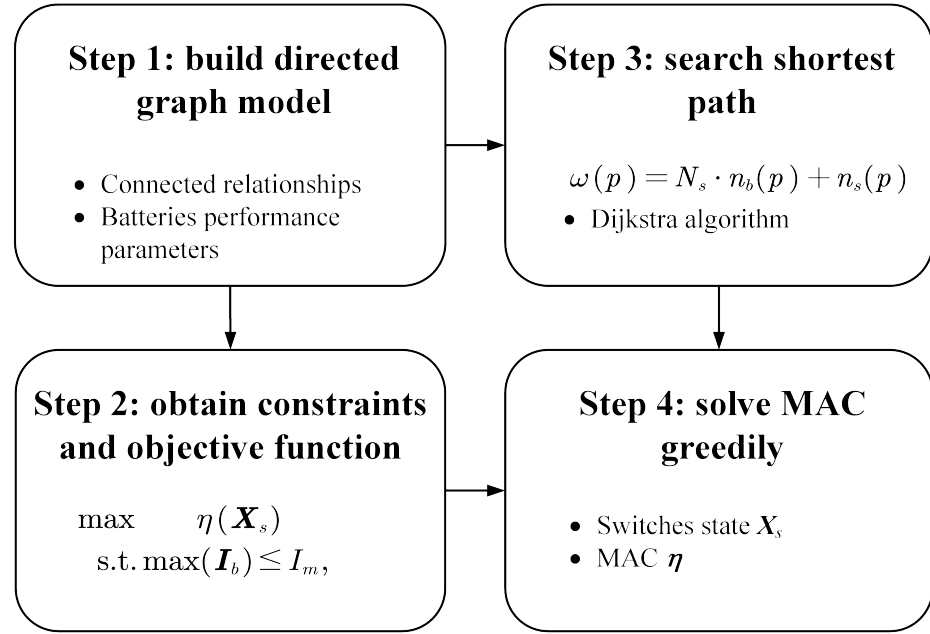


Figure 2: Diagram of this method, which contains four main steps.

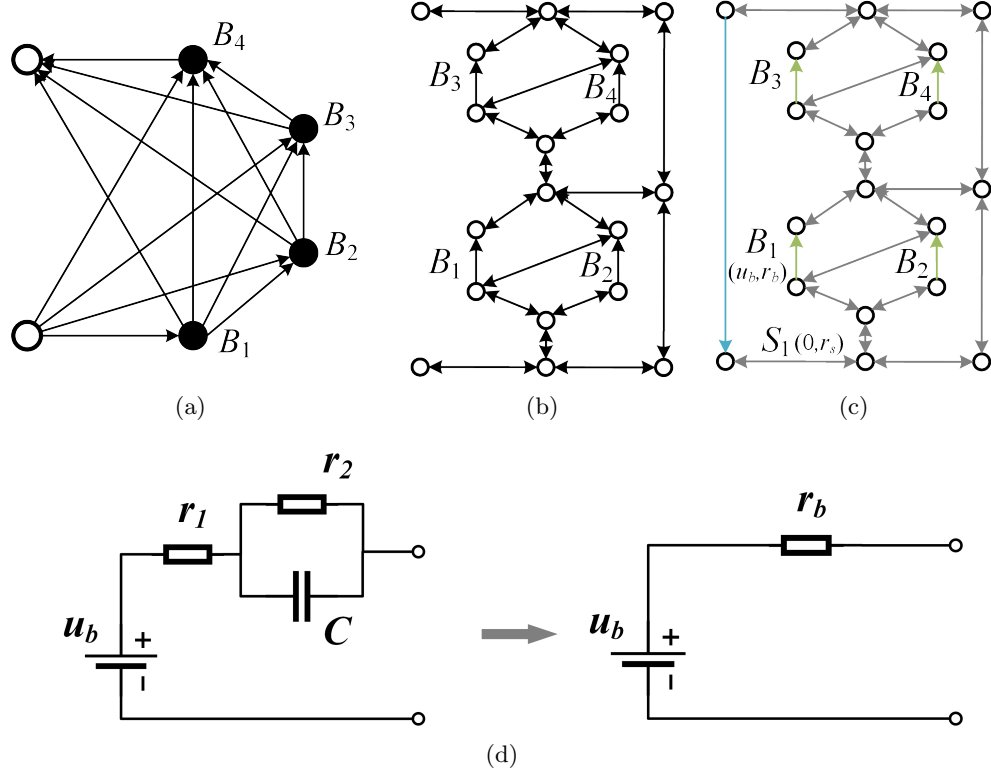


Figure 3: Directed graph models used in (a) He's work [20], (b) our previous work, and (c) [the improved model in](#) this paper. (d) The equivalent circuit of a battery in this method.

151 was able to accurately and comprehensively represent represents the RBS topological structure
 152 but could not cannot be used for quantitative MAC calculations due to the lack of consideration
 153 for battery and switch performance parameters because it does not consider the voltage, internal
 154 resistance, and MAC of the battery. To address this, an improved directed graph model is used here
 155 based on our original model, issue, we improve our previous model by adding electromotive force and
 156 resistance attributes on the edges based to equivalent circuits(Figure 3e)on its equivalent circuits.
 157 The model also considers the external load as an equivalent resistance and integrate integrates it
 158 into the analysis, making it a complete circuit model for later circuit analysis. The following will
 159 provide analyses. Fig. 3c shows the improved directed graph model used in this paper. The following
 160 provides a detailed explanation of the method for equating the components in RBS components in
 161 RBSs and constructing the directed graph model.

162 In order to To use circuit analysis methods to solve the MAC of the RBS, the components in the
 163 RBS are equated to ideal circuit elements. As shown in Figure For instance, as shown in Fig. 3d,
 164 the battery in the RBS can be is represented as a black-box circuit consisting of two resistors (i.e.,
 165 r_1 and r_2) and a capacitor (i.e., C), known as the Thevenin model [21, 22]. With an emphasis on
 166 the stable output of the RBS, the capacitor in the Thevenin model can be considered as an open
 167 circuit without affecting the steady-state current. Therefore, the battery is battery B_i in the RBS
 168 can be simplified as the a series connection between a constant voltage source u_i and a resistor r_i .
 169 Furthermore, the state of switch j - S_j in the RBS is represented by a binary variable x_j , where 0 is
 170 for ON and 1 is for OFF, respectively OFF. When the switch is closed, it-the circuit can be regarded
 171 as a resistor with a very small resistance value r_j . Lastly Finally, the external load is considered as
 172 a resistor with a value of resistance R_o .

173 For a given RBS structure, the its directed graph model for the RBS $G(V, E)$ is constructed as
 174 a directed graph $G(V, E)$ in such a way that follows:

- 175 Nodes: The nodes in the directed graph correspond to the connection points of components in
 176 the actual RBS. Assuming there are a total of N nodes in the RBS, for the sake of convenience,
 177 the anode of the RBS is denoted as v_1 and the cathode as v_N .
- 178 Edges: The edges in the directed graph correspond to the batteries, switches, and external
 179 electrical loads in the actual RBS. Therefore, there are three types of directed edges. For a
 180 battery B_i , its directed edge e_i is drawn from the cathode to the anode, as the battery because
 181 the battery in operation only allows current to flow in one direction when in operation. For
 182 a. For switch S_j , since it is allowed to work under bi-directional bidirectional currents, it
 183 is represented by a pair of directed edges with two-way directions. Regarding the external
 184 electronic load, as because it is connected to the anode and cathode of the RBS, a directed
 185 edge from v_N to v_1 is used to represent represents it. In conclusion, for a given RBS structure
 186 with N_b batteries and N_s switches, the total number of directed edges is $N_b + 2N_s + 1$, where
 187 1 refers to the external electrical load.
- 188 3. Edges' attributes Attributes of edges: Each edge is assigned two attributes, voltage difference
 189 and resistance, based on the equivalent method mentioned above. The values for the battery
 190 B_i , switch S_j , and external loads correspond to (u_i, r_i) , $(0, r_j)$, and $(0, R_o)$, respectively.

2.2 Constraints and Objective Function

Based on the definition of MAC, determining the MAC of RBS. For a given RBS, determining its MAC involves maximizing the RBS output current while ensuring that the currents of all batteries' battery currents do not exceed the batteries' maximum allowable current. In this subsection, MAC. This subsection establishes the constraints and objective function to solve determine the RBS's MAC will be established through circuit analysis, based on the previously constructed directed graph model provided in the previous section.

First, the topology in the directed graph model is represented in matrix form \mathbf{A} , known as the incidence matrix, to facilitate circuit analysis. The specific definition of the incidence matrix is shown in Equation 1, and defined as follows:

$$a_{kl} = \begin{cases} 1, & \text{edge } l \text{ leaves node } k, \\ -1, & \text{edge } l \text{ enters node } k, \\ 0, & \text{otherwise.} \end{cases} \quad (1)$$

For a directed graph consisting of N nodes and $N_b + 2N_s + 1$ directed edges, its incidence matrix \mathbf{A} is an $N \times (N_b + 2N_s + 1)$ matrix. In this matrix, the rows and columns represent the nodes and edges of the directed graph, respectively. By distinguishing the components in the RBS corresponding to each column, \mathbf{A} can be rewritten as :-

$$\mathbf{A} = [\mathbf{A}_b \quad \mathbf{A}_s \quad \mathbf{A}_o], \quad (2)$$

where \mathbf{A}_b , \mathbf{A}_s , and \mathbf{A}_o are the sub-matrices corresponding to the batteries, switches, and external electrical load, respectively. To alleviate reduce the computational complexity, the dimensions of matrix \mathbf{A} undergoes dimensionality reduction are reduced. Since each directed edge has one node to leave and one to enter, the sum of the values in every column of \mathbf{A} is sum to zero. Therefore removing any single one, removing the last row will not result in a loss of information. Without loss of generality, the last row is removed here. On the other hand, Conversely, since each switch in the RBS is represented by a pair of directed edges with two-way directions, the two columns corresponding to the switch are mutually opposite. Thus, for the sub-matrix \mathbf{A}_s , only one column is retained for each pair of columns representing the same switch. As a result, \mathbf{A} can be reduced to a an $(N - 1) \times (N_b + N_s + 1)$ matrix, denoted as $\tilde{\mathbf{A}}$, for further calculation of current and voltage. Similar to Equation 2 Eq. (2), $\tilde{\mathbf{A}}$ can be rewritten as :-

$$\tilde{\mathbf{A}} = [\tilde{\mathbf{A}}_b \quad \tilde{\mathbf{A}}_s \quad \tilde{\mathbf{A}}_o]. \quad (3)$$

After obtaining the incidence matrix, the currents of all batteries and output in the RBS are

²¹⁷ determined by solving the circuit equations. According to ~~Kirchhoffs law~~^{Kirchhoff's laws}, we have

$$\begin{cases} \tilde{\mathbf{A}}\mathbf{I} = \mathbf{0}, \\ \mathbf{U} = \tilde{\mathbf{A}}^T \mathbf{U}_n, \end{cases} \quad (4)$$

²¹⁸ where \mathbf{I} and \mathbf{U} indicate the current and voltage difference arrays of the $N_b + N_s + 1$ edges, respectively;
²¹⁹ ~~and~~ \mathbf{U}_n is the voltage array of the $N - 1$ nodes. These directed edges are treated as generalized
²²⁰ branches and expressed in matrix form as follows:²²¹

$$\mathbf{I} = \mathbf{Y} \mathbf{X} \mathbf{U} - \mathbf{Y} \mathbf{X} \mathbf{U}_s + \mathbf{I}_s, \quad (5)$$

²²¹ where \mathbf{U}_s and \mathbf{I}_s denote the source voltage and source current of the generalized branches, respec-
²²² tively. Because all batteries have been equivalent to voltage sources rather than current sources
²²³ in the previous subsection, all elements of the array \mathbf{I}_s are ~~0, while zero, whereas~~ the elements of
²²⁴ the array \mathbf{U}_s are equal to the first attribute of the corresponding edges in the directed graph. The
²²⁵ ~~matrix~~ \mathbf{Y} in ~~Eq. (5)~~ is the admittance matrix of the circuit, ~~and is~~ defined as the inverse of the
²²⁶ impedance matrix. ~~That is the elements of the diagonal. The elements on the diagonal of~~ matrix
²²⁷ \mathbf{Y} are equal to the reciprocal of the ~~resistance, which is the~~ second attribute of the corresponding
²²⁸ edges in the directed graph, ~~and the~~. ~~The~~ off-diagonal elements ~~are 0. The of~~ \mathbf{Y} ~~are zero.~~ \mathbf{X} is the
²²⁹ state matrix, ~~which describes that determines~~ whether the RBS batteries and switches ~~are allowed~~
²³⁰ ~~to can~~ pass current. It is defined as

$$\mathbf{X} = \text{diag}(\underbrace{1, 0, \dots, 1}_{N_b \text{ of } 0/1}, \underbrace{1, 0, \dots, 1}_{N_s \text{ of } 0/1}, 1) = \begin{bmatrix} \mathbf{X}_b & & \\ & \mathbf{X}_s & \\ & & 1 \end{bmatrix}, \quad (6)$$

²³¹ Where the elements where element x_i of the matrix \mathbf{X}_b represent whether the battery i indicates
²³² whether battery B_i has been removed from the circuit, with $x_i = 1$ indicating removal and $x_i = 0$
²³³ indicating that it battery B_i is still available to supply power. When all batteries are ~~health~~ healthy
²³⁴ and capable of providing current to the external load, \mathbf{X}_b is ~~an the~~ identity matrix. The elements
²³⁵ x_j of the matrix \mathbf{X}_s represent whether the switch j determine whether switch S_j is closed, with
²³⁶ $x_j = 1$ indicating ~~closure a closed switch~~ and $x_j = 0$ indicating ~~disconnection an open switch~~, which
²³⁷ is consistent with the previous subsection.

²³⁸ Theoretically, the output current I_o and the currents of each battery \mathbf{I}_b in the RBS can be
²³⁹ determined by solving ~~Equations 4, 5, and 6~~^{Eqs. (4)–(6)} under any given state \mathbf{X} . In order to
²⁴⁰ obtain specific constraint conditions and objective functions To further simplify the problem, it is
²⁴¹ further assumed that all batteries have the same electromotive force and internal resistance, denoted
²⁴² as which are denoted u_b and r_b , respectively. This allows for the derivation of us to derive explicit
²⁴³ expressions for I_o and \mathbf{I}_b . After derivation and simplification, the output current I_o and the currents
²⁴⁴ of each battery \mathbf{I}_b are ultimately represented as ~~Equations 7 and 8, respectively.~~ Eqs. (7) and (8),

245 respectively:

$$I_o = \frac{1}{R_o r_b} \tilde{\mathbf{A}}_o^T \mathbf{Y}_n^{-1}(\mathbf{X}) \tilde{\mathbf{A}}_o \mathbf{U}_b, \quad (7)$$

246

$$\mathbf{I}_b = \frac{1}{r_b^2} [\tilde{\mathbf{A}}_b^T \mathbf{Y}_n^{-1}(\mathbf{X}) \tilde{\mathbf{A}}_b \mathbf{U}_b - r_b \mathbf{U}_b], \quad (8)$$

247 where \mathbf{U}_b is a ~~a-an~~ $N_b \times 1$ array with all elements ~~equaling~~ equal to u_b , and \mathbf{Y}_n is the equivalent
248 admittance matrix of the circuit, and is defined as

$$\mathbf{Y}_n(\mathbf{X}) = \frac{1}{R_o} \tilde{\mathbf{A}}_o \tilde{\mathbf{A}}_o^T + \frac{1}{r_b} \tilde{\mathbf{A}}_b \mathbf{X}_b \tilde{\mathbf{A}}_b^T + \frac{1}{r_s} \tilde{\mathbf{A}}_s \mathbf{X}_s \tilde{\mathbf{A}}_s^T. \quad (9)$$

249 To characterize the current output capacity of the RBS structure under different switching states,
250 an indicator η is defined by the ratio of I_o and to $\max(\mathbf{I}_b)$ shown in Equation 10:

$$\eta = \frac{I_o}{\max(\mathbf{I}_b)}. \quad (10)$$

251 Finally the problem of solving finding the MAC can be formulated as

$$\max \eta(\mathbf{X}_s) \quad (11)$$

$$\text{s.t.s.t. } \max(\mathbf{I}_b) \leq I_m, \quad (12)$$

252 where I_m is the maximum allowable current MAC of the battery.

253 However, it is remains computationally difficult to solve 11 because of the Eq. (11) because of
254 \mathbf{Y}_n^{-1} . On one hand, due to the introduction of nonlinear terms by \mathbf{Y}_n^{-1} , many effective renders many
255 methods in linear optimization are not suitable unsuitable for this problem. On the other hand, the
256 rank of \mathbf{Y}_n is proportional to the number of batteries and switches, which can be very large for a
257 large RBS system, leading to a significant computational burden. Therefore As a result, intelligent
258 algorithms that rely on evolving evolution by iteration may face efficiency issues problems when
259 dealing with large RBS system. In order to a large RBS. To address this issue, the problem should
260 be considered from the perspective of guiding the RBS to reconstruct as many parallel structures
261 as possible. Consequently, a greedy algorithm based on the shortest path is proposed. The detailed
262 implementation process of this algorithm is presented in the following two subsections.

263 2.3 Shortest Pathpath

264 The path p used in this method is defined as the complete route that passes through one battery (or a
265 consecutive series of batteries) and closed switches, connecting the anode v_1 to the cathode v_N of the
266 RBS. By applying a penalty to the series-connected batteries on the path, where additional batteries
267 imply a longer greater distance, the algorithm encourages the RBS to form parallel structures as
268 much as possible. Meanwhile to the extent possible. In addition, to reduce the number of switches
269 controlled during the reconstruction process, a penalty is also applied to the total number of switches
270 on the path, while ensuring the minimum number of batteries. Therefore, the distance ω of the

271 path p is defined by the following equation:-

$$\omega(p) = N_s \cdot n_b(p) + n_s(p), \quad (13)$$

272 where N_s is the total number of switches in the system, and $n_b(p)$ and $n_s(p)$ are number of batteries
273 and switches in the path p , respectively. Moreover, the shortest path SP_i is defined as the path with
274 the minimum ω for battery i , as shown in the following equation B_i :

$$SP_i = \arg \min_{p \in P_i} \omega(p), \quad (14)$$

275 where P_i is the set of all paths from v_1 to v_N which pass through the that pass through directed
276 edge i .

277 The SP_i can be solved by the Dijkstra algorithm. The Dijkstra algorithm is a graph search
278 graph-search method that finds the shortest path between two given nodes in a weighted graph,
279 efficiently solving the single-source shortest-path problem. Assuming that shortest-path problem.
280 Denoting the cathode and anode of battery i are denoted B_i as v_i^- and v_i^+ respectively, the then
281 path p of battery i can be divided into three segments: $v_1 \rightarrow v_i^-$, $v_i^+ \rightarrow v_N$, and $v_i^- \rightarrow v_i^+$. The
282 $v_i^- \rightarrow v_i^+$ is the directed edge corresponding to battery i . With the Dijkstra algorithm, shortest
283 paths for $v_1 \rightarrow v_i^-$ and $v_i^+ \rightarrow v_N$ can be calculated under the weights given in Equation 13,
284 denoted as Eq. (13) and denoted $SP(v_i^- \rightarrow v_i^+)$ and $SP(v_i^+ \rightarrow v_N)$, respectively. Finally, the SP_i
285 for battery i is formed by the complete path with which consists of $SP(v_1 \rightarrow v_i^-)$, $v_i^- \rightarrow v_i^+$,
286 and $SP(v_i^+ \rightarrow v_N)$.

287 2.4 Greedy Algorithmalgorithm

288 From the perspective of series vs parallel connections, integrating more batteries into the circuit
289 through their shortest paths (SPs) results in a larger number of more batteries connected in
290 parallel, thereby increasing the total output current of the RBS. However, conflicts may arise be-
291 tween the SPs of different batteries. For instance, the SPs of two batteries might form
292 a short-circuited short-circuit RBS structure, which is not allowed. To address this issue, a greedy
293 algorithm is employed to incorporate as many SPs as possible while
294 satisfying the reconstruction requirements.

295 The algorithm, as illustrated in Figure 4, can be (see pseudo-code in Algorithm 1) is illustrated
296 in Fig. 4 and is summarized as follows, with the corresponding pseudo-code presented in Algorithm
297 1.: First, the shortest paths (SPs) are obtained using Equations 13 and 14. SPs are obtained by using
298 Eqs. (13) and (14) in conjunction with Dijkstra Searchthe Dijkstra search. Next, the matrix A is
299 calculated using Equation 1Eq. (1), and the initial N_{set} is set to N_b . The algorithm iteratively
300 checks uses a dichotomy method to iteratively check until convergence different combinations of c_b
301 batteries from N_b and updates N_{set} using a dichotomy method until convergence is reached N_{set} .
302 For each combination, the algorithm constructs an effective solution if possible, and calculates the
303 currents I_o and I_b using Equations 7 and 8 by using Eqs. (7) and (8). If the maximum current I_b is
304 less than or equal to I_m , the η is calculated using Equation 10 by using Eq. (10), and the maximum

305 η is updated accordingly. Finally, the algorithm outputs the maximum η once $N_{set} \approx N_{set}$ converges.

306 3 Case Study

307 3.1 Structures

308 Currently, two types of RBS structures have been proposed by Visairo et al. [11] and Lawson et al.
309 [15], both of which have ~~been applied in practice~~ seen real use. The primary goal of Visairo's structure
310 ([Figure 5b](#)) was to achieve dynamic adjustment of RBS output; however [Fig. 5b](#) is to dynamically
311 adjust the RBS output power. However, the isolation of unhealthy batteries ~~was~~ is not sufficiently
312 addressed. When batteries need to be isolated in the RBS of Visairo's structure, the methods
313 for isolating them and the subsequent changes in RBS output warrant further investigation in their
314 work. Lawson et al. conducted research on battery isolation in RBS and specifically designed the
315 designed the RBS structure shown in [Figure 5a](#). This structure has the advantage of easily isolating
316 batteries, but [Fig. 5a](#) to isolate batteries. Although this structure easily isolates batteries, it cannot
317 dynamically adjust the output current of the RBS. Based on the structures of Visairo and Lawson,
318 this paper presents a new structure, as shown in [Figure 5e](#), which combines the advantages of
319 both [proposes the structure shown in Fig. 5c](#). By integrating the Visairo RBS structure into the
320 Lawson RBS structure, the new proposed structure not only allows has the flexibility to switch
321 the batteries between series, parallel, and mixed series-parallel modes, but also easily enables but
322 also allows the isolation of highly degraded batteries from the RBS. And their variations in output
323 current under battery isolation conditions will be studied. This RBS structure will be used to
324 validate the effectiveness of the proposed method for calculating the MAC, and be compared with the
325 Lawson's and Visairo's structure to illustrate its advantage on battery isolation. These four-battery
326 RBS structures are investigated in the case study, including the scenarios with random isolated
327 batteries.

328 3.2 Result

329 As shown in [Figure Fig. 5c](#), the new RBS structure consists of 4 four batteries and 19 switches. The
330 [Figure 6a shows the](#) corresponding directed graph ~~is depicted in Figure 6a~~, which is composed of ~~of~~
331 ~~a total of~~ 18 nodes and 43 edges. Batteries B_1 , B_2 , B_3 , and B_4 are denoted by green directed edges
332 in the graph, while [and](#) the 19 switches are represented by gray directed edges with bi-directional
333 bidirectional arrows. The external electrical load is treated as a directed edge from the cathode of
334 the RBS (i.e., node 18) to the anode (i.e., node 1), as indicated by the blue directed edge in the
335 graph. Utilizing Equation 13 Using Eq. (13) and the Dijkstra algorithm, the ~~SPs~~ SPs of the four
336 batteries in the RBS structure of [Figure Fig. 5c](#) are highlighted ~~by red in Figures 6b–in red in Figs.~~
337 [6b and 6e](#). Finally, the ~~MAC calculation results~~ calculated MACs of the structure in [Figure 5c](#) are
338 shown as Table 1 and [Figure 6f](#). [Fig. 5c](#) are listed in Tab. 1 and shown in Fig. 6f, as obtained by
339 the greedy algorithm 1. Table Tab. 1 contains the ~~switches states~~ states of the switches, the output
340 current I_o , the battery current I_b and the ratio η of the RBS structure with all batteries in good

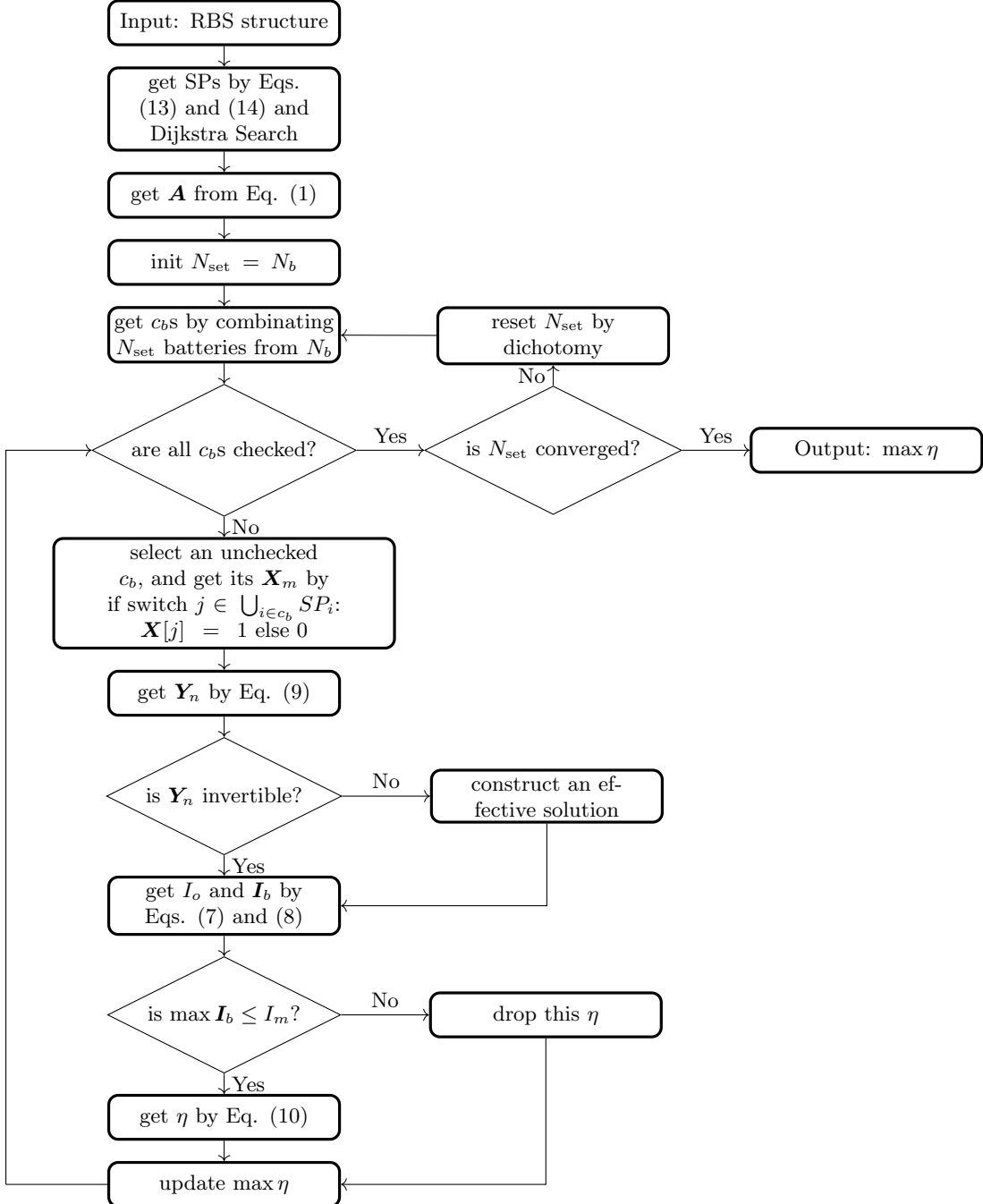


Figure 4: The computational flowchart of the MAC for a given RBS.

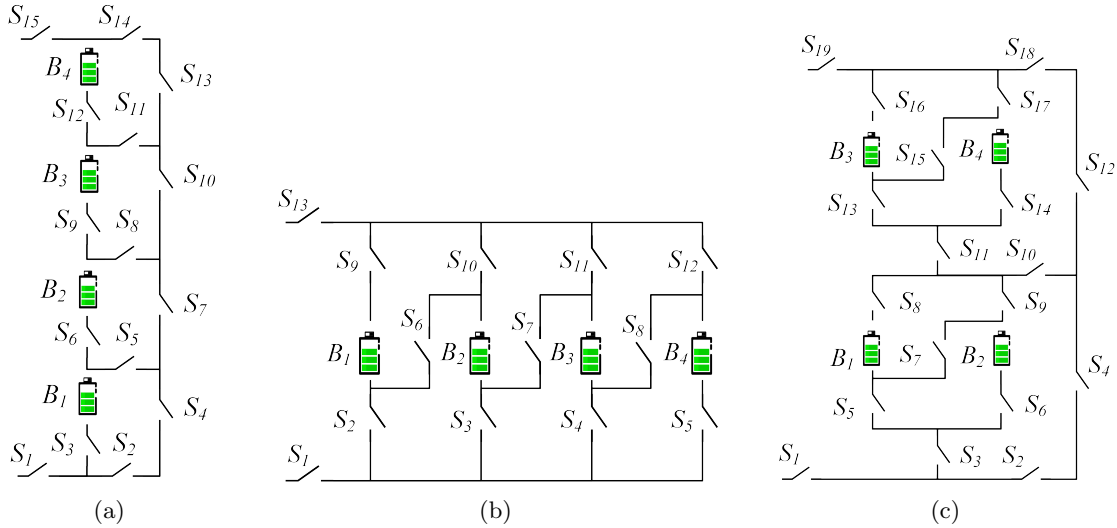


Figure 5: The 4-battery four-battery RBS structures proposed by (a) Lawson [15], (b) Visairo [11] and (c) this paper.

341 health when the RBS output reaches the MAC. Figure Fig. 6f presents the corresponding circuit,
342 with the red highlight indicating that the current is flowing through the respective branches.

Table 1: Calculated MAC Calculating result of the 4-battery for four-battery RBS structure in Figure Fig. 5c.

Structure	Figure 5c with 4four batteries and 19 switches
Switch ON-on	$S_1, S_3, S_5, S_6, S_8, S_9, S_{10}, S_{12}, S_{18}, S_{19}$
I_o	$2u_b/(2R_o + r_b)$
I_b	$[u_b/(2R_o + r_b), u_b/(2R_o + r_b), 0, 0]$
η_{\max}	2

343 Similarly, the MAC calculation results of the structures in Figures MAC calculation for the
344 structures in Figs. 5a and 5b are shown as Table 2 and Table listed in Tabs. 2 and 3, respectively.

345 To verify and compare the results from the greedy algorithm, we also used a brute-force algorithm
346 that iterates through all possible switch states to calculate the MAC of the same three RBSs. The
347 final results are the same as the results shown in Tabs. 1–3. The method uses the greedy algorithm
348 to calculate 11, 11, and 1 reconfigured structures for the RBS structure in Figs. 5c, 5a, and 5b,
349 respectively. For the same RBS, the method counts all possible switch states, which equates to 2^{19} ,
350 2^{15} , and 2^{13} structures, respectively.

351 Furthermore, the RBS under the scenario of with isolated batteries is taken into consideration
352 and calculated. The MAC calculation results for the three structures under study, with varying
353 numbers of isolated batteries, are presented in Table 4. Figures 7a–d illustrate the
354 corresponding switch-control schemes for the new structure proposed in this paper
355 under different isolated battery conditions. The characteristics of these three structures in the

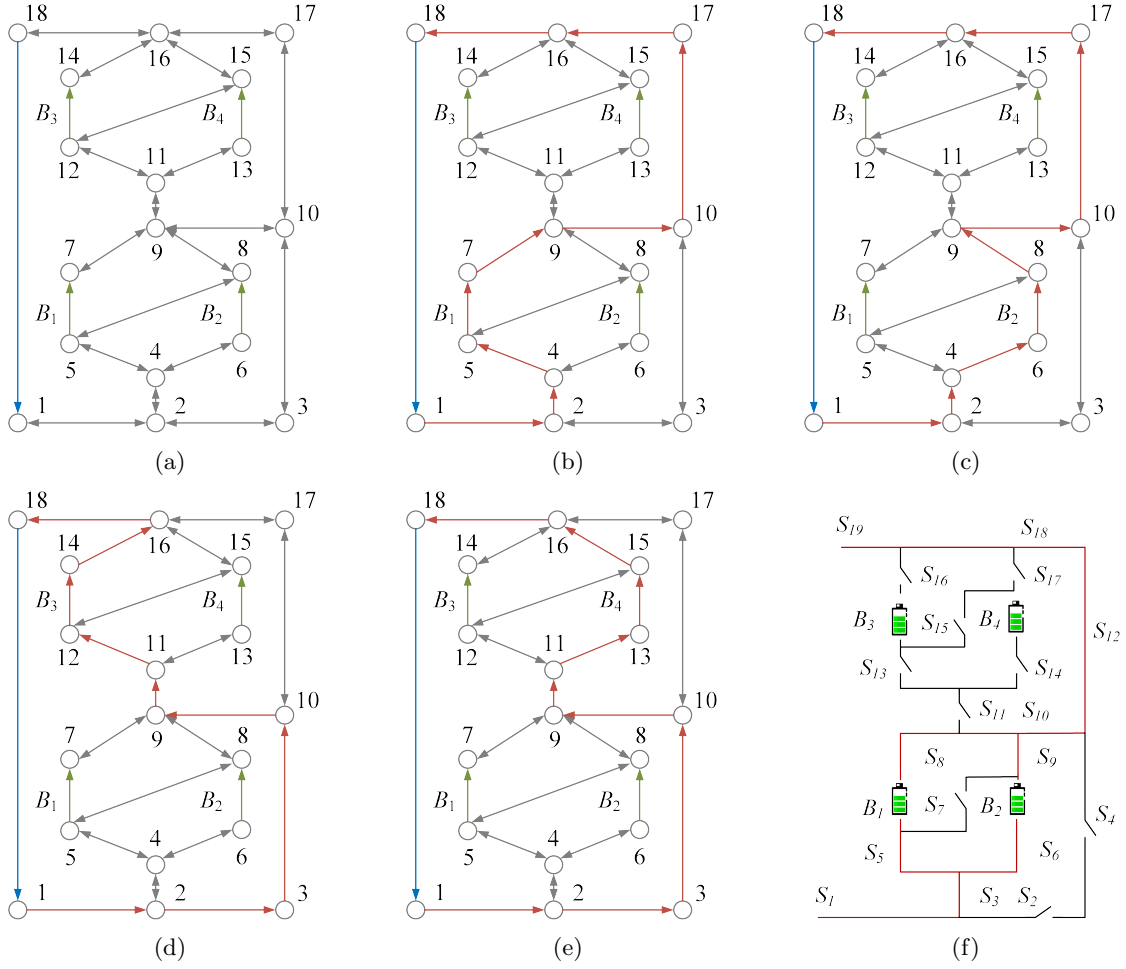


Figure 6: For the RBS structure in Figure Fig. 5c, (a) its directed graph and the ~~SPs~~ SPs (highlighted in red) of battery (b) B_1 , (c) B_2 , (d) B_3 , and (e) B_4 . (f) The circuit Circuit of the RBS with its output reaching the MAC.

Table 2: MAC Calculating result of the ~~4-battery~~ four-battery RBS structure in Figure Fig. 5a.

Structure	Figure 5a with 4 batteries and 15 switches
Switch ON	$S_1, S_3, S_5, S_7, S_{10}, S_{13}, S_{14}, S_{15}$
I_o	$u_b / (R_o + r_b)$
I_b	$[u_b / (R_o + r_b), 0, 0, 0]$
$\eta \max \eta$	1

Table 3: MAC Calculating result of the ~~4-battery~~ four-battery RBS structure in Figure Fig. 5b.

Structure	Figure 5b with 4 batteries and 13 switches
Switch ON	$S_1, S_2, S_3, S_4, S_5, S_9, S_{10}, S_{11}, S_{12}, S_{13}$
I_o	$4u_b / (4R_o + r_b)$
I_b	$[u_b / (4R_o + r_b), u_b / (4R_o + r_b), u_b / (4R_o + r_b), u_b / (4R_o + r_b)]$
$\eta \max \eta$	4

356 context of battery isolation will be discussed in the next subsection conditions of isolated batteries.

Table 4: The variation Variation of MAC with the number of isolated batteries for different RBS structures, including the structure proposed by Lawson et al., Visairo et al., and the structure proposed in this paper.

Number of isolated batteries	η of RBS structure		
	our This paper	Visairo	Lawson
0	2	4	1
1	2	3	1
2	2 ^a or 1 ^b	2	1
3	1	1	1

^a Isolate two batteries within the same substructure, as shown in Fig. 7b.

^b Isolate one battery in each of the two substructures, as shown in Fig. 7c.

357 3.3 Discussion

358 In this subsection, we firstly discuss the correctness of the results presented in Figure 6 and Table
 359 Consider first the results shown in Fig. 6f and listed in Tab. 1. When B_1 and B_2 or B_3 and B_4
 360 are connected in parallel, the RBS can output outputs the maximum current, which is $\eta = 2$, (i.e.,
 361 twice the current output of a single battery in the RBS). Adding more batteries to the main
 362 circuit can only form only forms a series structure and will does not improve the MAC. Therefore,
 363 the switches state given in Table 1 can make state of the switches given in Tab. 1 maximizes the
 364 RBS output current reach the maximum. The brute-force method, which go through all possible
 365 switch states, also gives the same result.

366 It is important to note that when solving for MAC The literature contains no report on an
 367 algorithm for calculating the MAC of an RBS. The brute-force algorithm, which goes through all
 368 possible switch states, is the most straightforward way to determine the MAC and is used as a
 369 benchmark for the proposed greedy algorithm. If an RBS has N_b batteries and N_s switches and the
 370 corresponding directed graph has N nodes, 2^{N_s} iterations are required to traverse all reconfigured
 371 structures. Calculating each reconfigured structure using Eqs. (7)–(10) requires matrix inversion and
 372 matrix multiplication, which has a time complexity of $O(N^3 + 2N^2N_b + N^2N_s + NN_b^2)$. Therefore,
 373 the time complexity of the brute-force algorithm is $O((N^3 + 2N^2N_b + N^2N_s + NN_b^2)2^{N_s})$. The
 374 greedy algorithm proposed in this paper requires that SP be found for each battery, which requires
 375 N_b iterations. Each SP can be obtained by several applications of Dijkstra's algorithms. Therefore,
 376 the total time complexity for calculating all SPs is $O(N_b(N_b + 2N_s)\log_{10} N)$. According to Appendix
 377 1, the RBS can reconfigure $C_{N_b}^{N_{set}}$ structures by selecting N_{set} batteries from N_b batteries, which gives
 378 $\sum_{N_{set}=1}^{N_b} C_{N_b}^{N_{set}} / N_b \approx 2^{N_b} N_b^{-1}$ on average. Thus, with the bisection method, the time complexity of
 379 the greedy algorithm is $O((N^3 + 2N^2N_b + N^2N_s + NN_b^2)2^{N_b} N_b^{-1} \log_{10} N_b + N_b(N_b + 2N_s)\log_{10} N)$.
 380 Based on currently proposed RBS structures [23, 24, 25, 26, 27, 28], the number N_b of batteries, N_s
 381 of switches, and N of nodes are quantitatively related as follows: $N_s \approx (3-5)N_b$, $N \approx N_s$. After
 382 simplifying, the time complexity of the method with greedy algorithm is $O(2^{N_b} N_s^2 \log_{10} N_b)$, while
 383 it is $O(2^{N_s} N_s^3)$ for the method with brute force algorithm. Therefore, as the RBS grows, especially

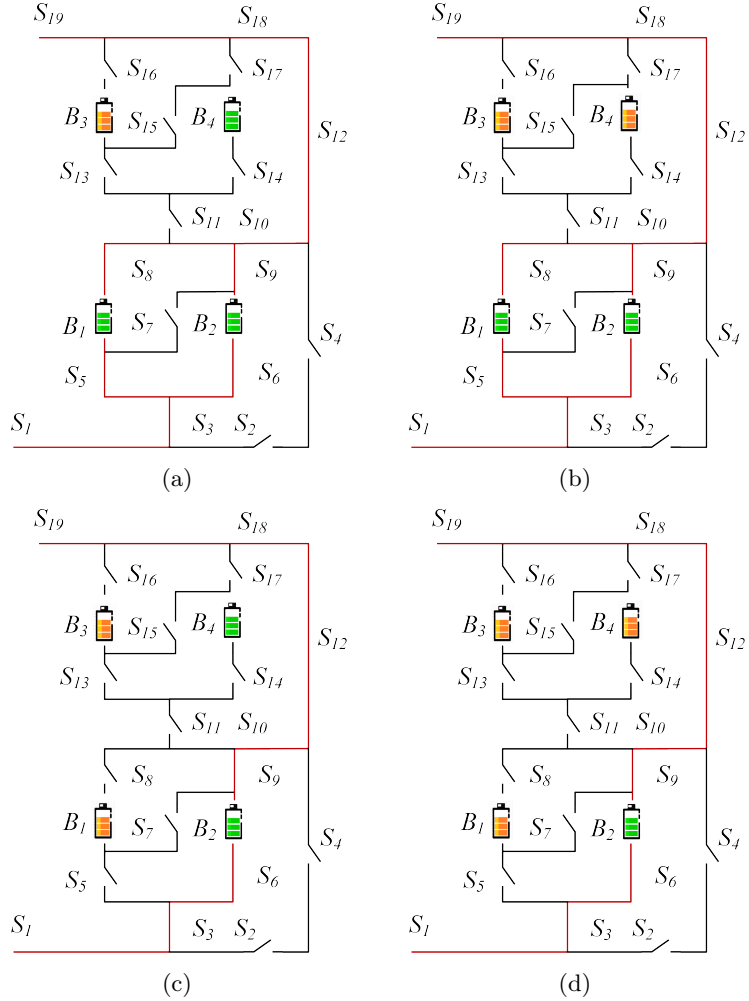


Figure 7: **The circuit** states of MACs when isolating (a) one, (b) two (best case), (c) two (worst case), and (d) three batteries for the structure in [Figure Fig. 5c](#).

384 in the number of switches, the greedy algorithm gains an advantage over the brute-force algorithm.
385 This is confirmed by the number of structures required to determine the MAC in the previous
386 section. Compared with the brute-force algorithm, the method based on the greedy algorithm is
387 3 000 to 48 000 times more efficient, which is theoretically $N_s 2^{N_s - N_b} \log_{10} N_b$ times according to the
388 above time-complexity analysis. This benefits from two key points:

- 389 (1) The SPs guide the RBS to reconfigure reasonable structures rather than blindly going through
390 all possible structures. This reduces the complexity from 2^{N_s} to 2^{N_b} , which is the main reason
391 for the improvement in efficiency.
- 392 (2) The bisection method further accelerates this process, reducing the complexity from 2^{N_b} to
393 $2^{N_b} N_B^{-1} \log_{10} N_b$.

394 However, the greedy algorithm proposed in this paper still contains exponential terms in the time
395 complexity, which means it may not be able to handle extremely large RBS structures having large
396 N_b .

397 Note that η is used as the objective function instead of I_o in solving for the MAC. This choice
398 makes the result of resulting MAC more reasonable. As shown in Table Tab. 1, I_o and I_b are
399 functions of R_o , u_b , and r_b . If However, when I_o were is used as the objective function, even for the
400 same RBS structure, the MAC result and corresponding switches state solution and corresponding
401 switch states could change due to different external electrical appliances. It This would increase
402 the difficulty and uncertainty in RBS structuredesign. In contrast, by using η as the objective
403 function, which is defined as the ratio of I_o and $\max I_b$, the influence of these factors on the results
404 can be eliminated. η solely reflects of designing the RBS structure. To eliminate this problem,
405 the maximum output current capability of the RBS structureratio $\eta = I_o / \max I_b$ is adopted as the
406 objective function in our research. Recall that η reflects only the structure's ability to output current,
407 rather than the actual current outputing by the battery system. Assuming that the maximum
408 allowed current MAC of batteries in the RBS is I_m , the maximum output current of the RBS
409 structure can be calculated as ηI_m by determining the η of the structure. Therefore, compared to
410 I_o , value of η is more suitable for structure designfor the structure.

411 The method proposed in this paper is significant for facilitates the design of next-generation RBSs
412 in the following aspects. Most of the ways: Most currently proposed RBS structures [23, 24, 25,
413 26, 27, 28] exhibit have simple topological characteristics, and the calculation of so calculating the
414 MACs is relatively straightforward, even intuitive. However, these simple structures do not always
415 fully satisfy the requirements of complex applications, such as dynamically adapting the circuit to
416 variable and random operating conditions ,and or actively equalizing differences among the between
417 batteries in the RBS. Moreover, isolating the batteries disrupts the original regularity and symmetry
418 of the topology, which complicates the otherwise simple structure, and the maximum output current
419 of the system becomes more challenging to obtain. Owing to the advantages of pervasiveness and
420 automationIn contrast, the proposed method can be employed to calculate calculates the MAC of
421 arbitrary RBS structures, which helps to address the aforementioned issues and paves the way for
422 more notably the complex and flexible RBS structure designstructures.

423 To illustrate this point, the MACs of the three RBS structures mentioned above are calculated
 424 after isolating one or more of the batteries, as shown in Table Tab. 4.
 425 Specifically, for the structure presented in Figure Fig. 5c, the corresponding circuit states of for the
 426 MACs when isolating different numbers of one to three batteries are depicted in Figures 7a–Figs.
 427 7a–7d. This structure has two cases of isolating two batteries in which two batteries are isolated:
 428 one is to isolate two batteries within the same substructure (Figure Fig. 7b), in which case $\eta = 2$;
 429 the other is to isolate one battery in each of the two substructures (Figure Fig. 7c), in which case
 430 $\eta = 1$. From the results, it can be observed The results in Figs. 7a–7d show that the proposed
 431 method provides reasonable outcomes for isolating batteries with any number and position.

432 any number of batteries in any position. Furthermore, the performance of output current for
 433 the three RBS when isolating RBSs with isolated batteries is also shown in Table Tab. 4. For the
 434 structure proposed by Lawson et al., the MAC remains the same as that without isolated battery
 435 cells, i.e., $\eta = 1$, when the is independent of the number of isolated battery cells increases, until all
 436 the cells in the RBS are isolated. For batteries. However, for Visairo's structure, the MAC decreases
 437 as upon increasing the number of isolated battery cells increases, until $\eta = 0$. In contrast batteries.
 438 Nevertheless, the MAC of the structure proposed in this work is positioned between the falls between
 439 the MACs of these two structures. This result indicates that the structure proposed in this paper
 440 , compared to Lawson's structure, has a larger MAC under than Lawson's for the same number of
 441 batteries , which means a wider output current regulation range . On the other hand, by simply
 442 changing the states of S_2 , S_4 , S_{11} , and S_{12} in the conversion structure, this structure can address the
 443 majority of battery isolation scenarios, whereas Visairo's structure requires specific battery targeting
 444 and switch control. In summary, the structure proposed in this paper has the advantages of both
 445 Lawson's and Visairo's structures and has a wider range of regulation of the output current.

4 Conclusion

446 This paper proposes a pervasive and automatical method for computing automated method to
 447 efficiently compute the MAC of the given an RBS. The method is implemented by a greedy algorithm
 448 combined with a an improved directed graph model, whose effectiveness is tested on a novel and
 449 complex RBS structure. The method remains effective for the application scenario of RBS battery
 450 isolation and demonstrates that the novel structure has the advantage on flexible output current and
 451 convenient battery isolation. Future research could focus on developing new indicators to evaluate
 452 the performance . Not only does the method provides the same global MAC calculation results as
 453 the brute force method, but it also improves the calculation efficiency by 3 000 to 48 000 times for
 454 three RBS structures in the case study. Theoretically, for an RBS with N_s switches and N_b batteries,
 455 the efficiency of the proposed method is $N_s 2^{N_s - N_b} \log_{10} N_b$ times that of the brute-force method,
 456 which is mainly because of using the batteries' SPs to guide the RBS to reconfigure reasonable
 457 structures rather than blindly going through all possible structures. The main advantage of this
 458 method is its ability to calculate the MAC of RBSs with arbitrary structures. Even in scenarios
 459 with random isolated batteries, the proposed method remains effective. This method helps to fully
 460 tap the current output potential of the RBS with the currents and voltages obtained by the method,

462 as well as modifying the equivalent model of the battery to allow for more accurate simulations of
 463 the RBS, including transient analysis, guide the RBS structure design and optimization in the design
 464 stage, and assist in evaluating the current-overload risk of the system in practical applications.

465 5 Appendix

Algorithm 1: Get the max available currents of a certain RBS

Data: Directed graph model $G(V, E)$ of the RBS
Result: $\max \eta$

```

1 for  $i \in E_b$  do
2    $P_i \leftarrow \{path|starts at v_1 and ends at v_n\};$ 
3    $SP_i \leftarrow p_i$  which has the minimum  $\omega(p_i)$  among all  $p_i \in P_i$ .
4 end
5 get  $A$  by Equation Eq. 1;
6 while not yet determine  $\max \eta$  do
7    $N_{set} \leftarrow$  number of setected SPs calculated by dichotomy;  $N_{set} \leftarrow$  number of setected SPs
      calculated by dichotomy;
8    $C_b \leftarrow$  set of all combinations of  $N_{set}$  batteries from  $N_b$ ;  $C_b \leftarrow$  set of all combinations of
       $N_{set}$  batteries from  $N_b$ ;
9   for  $c_b \in C_b$  do
10     $x_s \leftarrow$  list of all switches' state:  $x_s[j] = 1$  if  $j \in \bigcup_{i \in c_b} SP_i$  else 0;
11     $X \leftarrow diag[1, 1, \dots, 1, x_s];$ 
12    get  $Y_n$  by Eq. 9;
13    if  $Y_n$  is invertible then
14      | pass
15    else
16      | construct an effective solution
17    end
18    get  $I_o$  by Eq. 7;
19    get  $I_b$  by Eq. 8;
20    if  $\max(I_b) \leq I_m$  then
21      |  $\eta \leftarrow I_o / \max(I_b);$ 
22    else
23      | break
24    end
25  end
26 end

```

466 **Acknowledgments**

467 **Author Contributions**

468 B. Xu conceived the main idea, formulated the overarching research goals and aims, designed the
 469 algorithm, and reviewed and revised the manuscript. G. Hua developed and analyzed the model,
 470 implemented the code and supporting algorithms, and wrote the initial draft. C. Qian provided

471 critical review, commentary, and revisions. Q. Xia contributed to shaping the research, analysis,
472 and manuscript. B. Sun conducted the research and investigation process. Y. Ren secured the
473 funding and supervised the project. Z. Wang verified the results and provided necessary resources.

474 Funding

475 This work was supported by the National Natural Science Foundation of China (NSFC, No.52075028).

476 Conflicts of Interest

477 The authors declare that there is no conflict of interest regarding the publication of this article.

478 Data Availability

479 This work does not require any data to be declared or publicly disclosed.

480 References

- 481 [1] Yuqing Yang, Stephen Bremner, Chris Menictas, and Merlinde Kay. Battery energy storage
482 system size determination in renewable energy systems: A review. *Renewable and Sustainable
483 Energy Reviews*, 91:109–125, August 2018.
- 484 [2] Luanna Maria Silva de Siqueira and Wei Peng. Control strategy to smooth wind power output
485 using battery energy storage system: A review. *Journal of Energy Storage*, 35:102252, March
486 2021.
- 487 [3] Eugene Schwanbeck and Penni Dalton. International Space Station Lithium-ion Batteries for
488 Primary Electric Power System. In *2019 European Space Power Conference (ESPC)*, pages 1–1.
489 IEEE, September 2019.
- 490 [4] Lihua Zhang. Development and Prospect of Chinese Lunar Relay Communication Satellite.
491 *Space: Science & Technology*, 2021, January 2021.
- 492 [5] Jaephil Cho, Sookyung Jeong, and Youngsik Kim. Commercial and research battery
493 technologies for electrical energy storage applications. *Progress in Energy and Combustion
494 Science*, 48:84–101, June 2015.
- 495 [6] Naixing Yang, Xiongwen Zhang, BinBin Shang, and Guojun Li. Unbalanced discharging and
496 aging due to temperature differences among the cells in a lithium-ion battery pack with parallel
497 combination. *Journal of Power Sources*, 306:733–741, February 2016.
- 498 [7] Fei Feng, Xiaosong Hu, Lin Hu, Fengling Hu, Yang Li, and Lei Zhang. Propagation
499 mechanisms and diagnosis of parameter inconsistency within Li-Ion battery packs. *Renewable
500 and Sustainable Energy Reviews*, 112:102–113, September 2019.

- 501 [8] J. A. Jeevarajan and C. Winchester. Battery Safety Qualifications for Human Ratings. *Interface*
 502 *magazine*, 21(2):51–55, January 2012.
- 503 [9] Daniel Vázquez Pombo. A Hybrid Power System for a Permanent Colony on Mars. *Space:*
 504 *Science & Technology*, 2021, January 2021.
- 505 [10] Weiji Han, Torsten Wik, Anton Kersten, Guangzhong Dong, and Changfu Zou.
 506 Next-Generation Battery Management Systems: Dynamic Reconfiguration. *IEEE Industrial*
 507 *Electronics Magazine*, 14(4):20–31, December 2020.
- 508 [11] H. Visairo and P. Kumar. A reconfigurable battery pack for improving power conversion
 509 efficiency in portable devices. In *2008 7th International Caribbean Conference on Devices,*
 510 *Circuits and Systems*, pages 1–6. IEEE, April 2008.
- 511 [12] Song Ci, Jiucai Zhang, Hamid Sharif, and Mahmoud Alahmad. A novel design of adaptive
 512 reconfigurable multicell battery for power-aware embedded networked sensing systems. In *IEEE*
 513 *GLOBECOM 2007-IEEE Global Telecommunications Conference*, pages 1043–1047. IEEE,
 514 2007.
- 515 [13] Jan Engelhardt, Tatiana Gabderakhmanova, Gunnar Rohde, and Mattia Marinelli.
 516 Reconfigurable stationary battery with adaptive cell switching for electric vehicle fast-charging.
 517 In *2020 55th International Universities Power Engineering Conference (UPEC)*, pages 1–6,
 518 2020.
- 519 [14] Jan Engelhardt, Jan Martin Zepter, Tatiana Gabderakhmanova, Gunnar Rohde, and Mattia
 520 Marinelli. Double-string battery system with reconfigurable cell topology operated as a fast
 521 charging station for electric vehicles. *Energies*, 14(9):2414, 2021.
- 522 [15] Barrie Lawson. A Software Configurable Battery. *EVS26 International Battery, Hybrid and*
 523 *Fuel Cell Electric Vehicle Symposium*, 2012.
- 524 [16] Liang He, Linghe Kong, Siyu Lin, Shaodong Ying, Yu Gu, Tian He, and Cong Liu.
 525 Reconfiguration-assisted charging in large-scale lithium-ion battery systems. In *2014*
 526 *ACM/IEEE International Conference on Cyber-Physical Systems (ICCP)*, pages 60–71. IEEE,
 527 2014.
- 528 [17] Hahnsang Kim and Kang G Shin. On dynamic reconfiguration of a large-scale battery system.
 529 In *2009 15th IEEE Real-Time and Embedded Technology and Applications Symposium*, pages
 530 87–96. IEEE, 2009.
- 531 [18] Weiji Han, Anton Kersten, Changfu Zou, Torsten Wik, Xiaoliang Huang, and Guangzhong
 532 Dong. Analysis and estimation of the maximum switch current during battery system
 533 reconfiguration. *IEEE Transactions on Industrial Electronics*, 69(6):5931–5941, 2021.
- 534 [19] Si-Zhe Chen, Yule Wang, Guidong Zhang, Le Chang, and Yun Zhang. Sneak Circuit Theory
 535 Based Approach to Avoiding Short-Circuit Paths in Reconfigurable Battery Systems. *IEEE*
 536 *Transactions on Industrial Electronics*, 68(12):12353–12363, 2021.

- 537 [20] Liang He, Lipeng Gu, Linghe Kong, Yu Gu, Cong Liu, and Tian He. Exploring Adaptive
 538 Reconfiguration to Optimize Energy Efficiency in Large-Scale Battery Systems. In *2013 IEEE*
 539 *34th Real-Time Systems Symposium*, pages 118–127, December 2013.
- 540 [21] Hongwen He, Rui Xiong, Xiaowei Zhang, Fengchun Sun, and JinXin Fan. State-of-Charge
 541 Estimation of the Lithium-Ion Battery Using an Adaptive Extended Kalman Filter Based on
 542 an Improved Thevenin Model. *IEEE Transactions on Vehicular Technology*, 60(4):1461–1469,
 543 May 2011.
- 544 [22] S.M. Mousavi G. and M. Nikdel. Various battery models for various simulation studies and
 545 applications. *Renewable and Sustainable Energy Reviews*, 32:477–485, April 2014.
- 546 [23] Song Ci, Jiucai Zhang, Hamid Sharif, and Mahmoud Alahmad. A Novel Design of Adaptive
 547 Reconfigurable Multicell Battery for Power-Aware Embedded Networked Sensing Systems. In
 548 *IEEE GLOBECOM 2007-2007 IEEE Global Telecommunications Conference*, pages 1043–1047,
 549 November 2007.
- 550 [24] Mahmoud Alahmad, Herb Hess, Mohammad Mojarradi, William West, and Jay Whitacre.
 551 Battery switch array system with application for JPL’s rechargeable micro-scale batteries.
 552 *Journal of Power Sources*, 177(2):566–578, March 2008.
- 553 [25] Hahnsang Kim and Kang G. Shin. Dependable, efficient, scalable architecture for management
 554 of large-scale batteries. In *Proceedings of the 1st ACM/IEEE International Conference*
 555 *on Cyber-Physical Systems*, ICCPS ’10, pages 178–187, New York, NY, USA, April 2010.
 556 Association for Computing Machinery.
- 557 [26] Younghyun Kim, Sangyoung Park, Yanzhi Wang, Qing Xie, Naehyuck Chang, Massimo
 558 Poncino, and Massoud Pedram. Balanced reconfiguration of storage banks in a hybrid electrical
 559 energy storage system. In *2011 IEEE/ACM International Conference on Computer-Aided*
 560 *Design (ICCAD)*, pages 624–631, November 2011.
- 561 [27] Taesic Kim, Wei Qiao, and Liyan Qu. A series-connected self-reconfigurable multicell
 562 battery capable of safe and effective charging/discharging and balancing operations. In *2012*
 563 *Twenty-Seventh Annual IEEE Applied Power Electronics Conference and Exposition (APEC)*,
 564 pages 2259–2264, February 2012.
- 565 [28] Liang He, Linghe Kong, Siyu Lin, Shaodong Ying, Yu Gu, Tian He, and Cong Liu.
 566 Reconfiguration-assisted charging in large-scale Lithium-ion battery systems. In *2014*
 567 *ACM/IEEE International Conference on Cyber-Physical Systems (ICCPs)*, pages 60–71, April
 568 2014.

¹ Maximum Allowable Current Determination of RBS By Using
² a Directed Graph Model and Greedy Algorithm

³ Binghui Xu^{1†}, Guangbin Hua^{1†}, Cheng Qian^{1*}, Quan Xia^{1,2}, Bo Sun¹, Yi Ren¹, and
⁴ Zili Wang¹

⁵ ¹School of Reliability and Systems Engineering, Beihang University, Beijing, 100191,
⁶ China

⁷ ²School of Aeronautic Science and Engineering at Beihang University, Beijing, China

⁸ *Address correspondence to: cqian@buaa.edu.cn

⁹ [†]These authors contributed equally to this work.

10

Abstract

11

Reconfigurable battery systems (RBSs) present a promising alternative to traditional battery systems due to their flexible and dynamically changeable topological structure that can be adapted to different battery charging and discharging strategies. During RBS operation, a critical system parameter known as the maximum allowable current (MAC) become pivotal. This parameter is instrumental in maintaining the current of each individual battery within a safe range and serves as a guiding indicator for the system's reconfiguration, thereby ensuring its safety and reliability. This paper proposes a method to calculate the MAC of arbitrary RBSs using a greedy algorithm in conjunction with a directed graph model of the RBS. By introducing the shortest path of the battery, the greedy algorithm transforms the enumeration of switch states in the brute-force algorithm into the combination of the shortest paths, which greatly increases the efficiency with which the MAC is determined. The directed graph model, based on the equivalent circuit, provides a specific method for calculating the MAC of a given structure. The proposed method is validated on two published four-battery-RBSs and one with a more complex structure. The results are the same as those of the brute-force algorithm, but the proposed method significantly improves the computational efficiency ($N_s 2^{N_s - N_b} \log_{10} N_b$ times faster than the brute force algorithm for an RBS with N_b batteries and N_s switches, theoretically). The main advantage of the proposed method is its ability to calculate the MAC of RBSs with arbitrary structures, even in scenarios with random isolated batteries.

29

1 Introduction

30

Battery energy storage systems (BESSs) are extensively used in various applications [1], such as wind power plants [2] and space power systems [3, 4], to store and release high-quality electrical energy

[5]. Typically, a BESS consists of numerous batteries interconnected by series-parallel circuitry to provide the required capacity storage. However, traditional BESSs, in which the batteries are connected in a fixed topology, suffer from a significant weakness in their worst battery due to the so-called cask effect. Moreover, if the worst battery fails during operation, it is highly likely to exacerbate the degradation of the other batteries, leading to reliability and safety issues [6, 7, 8]. These problems have become significant technical barriers in many engineering projects requiring high reliability, such as developing new-generation space vehicles [9].

Reconfigurable battery systems (RBSs), which can dynamically switch as required to different circuit topologies, are expected to solve this problem [10]. The switching circuit helps to isolate unhealthy batteries, thereby improving the safety and reliability of the battery system. To illustrate the working principle of an RBS, we consider a typical RBS structure developed by Visairo [11] (Fig. 1a), which is taken as an example to show the reconfiguration process. In this structure, the batteries can be connected not only in series when the switches $S_1, S_5, S_6, S_7, S_8, S_9$, and S_{13} are closed (see Fig. 1b) but also in parallel when $S_1, S_2, S_3, S_4, S_5, S_9, S_{10}, S_{11}, S_{12}$, and S_{13} are closed (Fig. 1c). Furthermore, when an unhealthy battery, for instance, the orange one B_3 in Fig. 1d, appears in the RBS, it can be isolated by opening its two adjacent switches (i.e., S_4 and S_{11}), ensuring that the system remains in a reliable working mode.

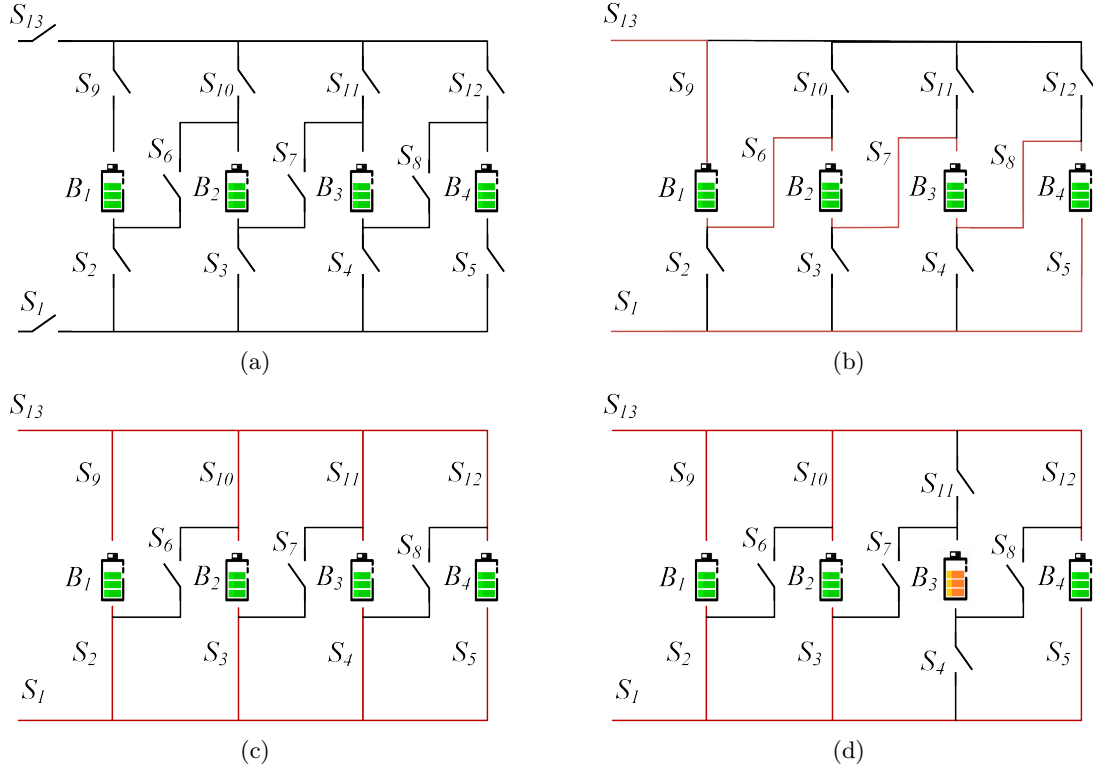


Figure 1: (a) The RBS structure proposed by Visairo[11], with all batteries in (b) series connection, (c) parallel connection, and (d) battery B_3 isolated.

Recently, various types of RBSs with different flexibility and reconfigurability have been de-

signed to meet application requirements. For example, Ci et al. [12] proposed an RBS structure that dynamically adjusts the battery discharge rate to fully exploit the available capacity of each battery. Jan's [13, 14] structures reconfigure structures with variant batteries in series to reach the (constantly changing) voltage requirements during electric vehicle charging. As shown in Fig. 1a, the structure proposed by Visairo et al. [11] changes the system's output voltage based on the load conditions, thereby reducing the power loss of the voltage regulator during the power supply process and improving the efficiency of energy use. Also, to enhance the energy efficiency of the system, Lawson et al. [15] and He et al. [16] proposed simplified structures that have fewer switches than Visairo's design. Kim et al. [17] improved the system's ability to recover from battery failures by introducing multiple ports into the structure.

The complex structure between batteries and switches gives RBSs flexibility but also creates challenges in the design and control of the system. Thus, several approaches to analyze the RBS structure and performance have been proposed to tackle these challenges. For instance, Han et al. [18] derived an analytical expression for the maximum switch current during battery system reconfiguration for a specific RBS structure. This helps guide the selection of switches and supports the design of RBS hardware. Chen et al. [19] proposed a systematic approach based on sneak circuit theory to fundamentally avoid the short-circuit problem of RBSs: They thoroughly analyzed all paths between the cathode and anode of each battery in the RBS and identified paths that only contain switches as short-circuit paths for pre-checking before system reconfiguration.

In spite of the maximum switch current mentioned above, the maximum allowable current (MAC), defined as the maximum allowed current under the constraints of the battery cell, is another critical indicator of RBSs that needs to be evaluated during the design or control of the system. The MAC helps the designers assess whether the RBS meets the output current requirements and contributes to the formulation of appropriate and safe management strategies for the battery management system. Unfortunately, few studies have analyzed the RBS structure to determine the RBS MAC. An intuitive and straightforward method is to enumerate all possible switch states and calculate the output current of the system under each reconfigured structure. However, this method is inefficient and time-consuming, especially for RBSs with a large number of switches.

To solve this issue, this paper proposes an efficient method to evaluate the MAC of RBSs. In this method, a greedy algorithm is designed to efficiently search the possible circuit topology of RBSs with MAC. This algorithm transforms the enumeration of switch states in the brute-force algorithm into the combination of the batteries' shortest paths. An improved direct graph model that considers the voltage, the internal resistance, the MAC of the battery, and the external load is also introduced to analyze the current of the RBS. The main contributions of this paper can be summarized as follows:

- An efficient method is proposed to determine the MAC of RBSs with arbitrary structures, including scenarios with isolated batteries.
- A greedy algorithm is applied to solve the MAC problem, the computational complexity of which is greatly reduced compared with the brute-force algorithm.
- An improved directed graph model is introduced to provide a specific method for calculating

90 the MAC of a given structure.

91 The remainder of this paper is organized as follows: Section II presents the framework and details
92 of the proposed directed graph model and greedy algorithm. Section III discusses a case study that
93 uses the proposed method to determine the MACs of two published four-battery RBSs and one with
94 a more complex structure. The calculation results, the algorithm's computational complexity, and
95 scenarios such as battery random isolation are also discussed. Finally, the concluding remarks are
96 presented in Section IV.

97 **2 Methodology**

98 The central principle of this method is to connect the batteries in an RBS in parallel to the ex-
99 tent possible, thereby maximizing the output current of the RBS. To achieve this universally and
100 automatically, the overall process is divided into the four steps shown in Fig. 2. First, a directed
101 graph model is established for subsequent computations. The model not only contains the con-
102 nected relationships between batteries and switches but also retains the performance parameters of
103 the batteries. Subsequently, based on the equivalent circuit, the MAC problem is transformed into
104 specific objective functions and constraints. The shortest paths (SPs, where additional batteries
105 and switches on the path are penalized as distance) for the batteries are then obtained by using the
106 Dijkstra algorithm to connect the batteries in the RBS in parallel. Finally, a greedy algorithm is
107 used to organize the switches, allowing the batteries to connect via their SPs while satisfying the
108 constraints, resulting in the MAC of the RBS.

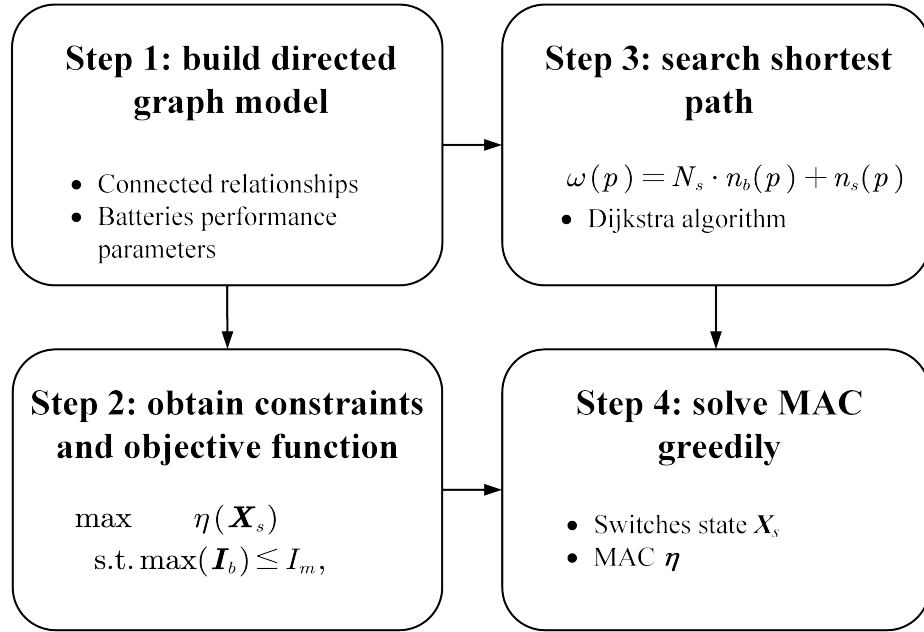


Figure 2: Diagram of this method, which contains four main steps.

¹⁰⁹ **2.1 Directed graph model**

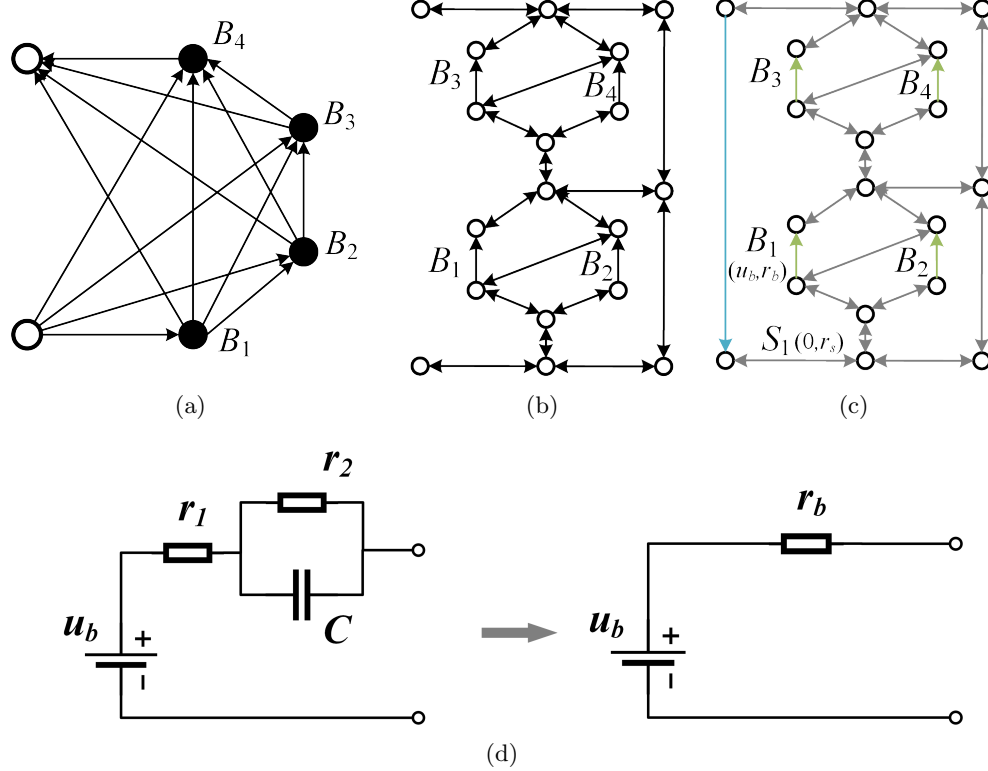


Figure 3: Directed graph models used in (a) He's work [20], (b) our previous work, and (c) the improved model in this paper. (d) The equivalent circuit of a battery in this method.

¹¹⁰ He et al. [20] proposed an abstracted directed graph model for an RBS, where the nodes represent
¹¹¹ the batteries, the edges represent the configuration flexibility, and the weight of each vertex corre-
¹¹² sponds to the battery voltage (Fig. 3a). The model captures all potential system configurations and
¹¹³ offers a direct metric for configuration flexibility, but it does not specify the physical implementa-
¹¹⁴ tion of the connectivity between batteries, meaning that one graph might correspond to multiple RBS
¹¹⁵ structures. We previously proposed a directed graph model that differs completely from He's model
¹¹⁶ by using nodes to represent the connections between batteries and switches and directed edges to
¹¹⁷ represent batteries and switches (Fig. 3b), allowing for a one-to-one correspondence between the
¹¹⁸ RBS structure and the directed graph model. This model accurately and comprehensively represents
¹¹⁹ the RBS topological structure but cannot be used for quantitative MAC calculations because it does
¹²⁰ not consider the voltage, internal resistance, and MAC of the battery. To address this issue, we im-
¹²¹ prove our previous model by adding electromotive force and resistance attributes on the edges based
¹²² on its equivalent circuits. The model also considers the external load as an equivalent resistance
¹²³ and integrates it into the analysis, making it a complete circuit model for later circuit analyses. Fig.
¹²⁴ 3c shows the improved directed graph model used in this paper. The following provides a detailed
¹²⁵ explanation of the method for equating components in RBSs and constructing the directed graph

126 model.

127 To use circuit analysis methods to solve the MAC of the RBS, the components in the RBS are
128 equated to ideal circuit elements. For instance, as shown in Fig. 3d, the battery in the RBS is
129 represented as a black-box circuit consisting of two resistors r_1 and r_2 and a capacitor C , known as
130 the Thevenin model [21, 22]. With an emphasis on the stable output of the RBS, the capacitor in
131 the Thevenin model can be considered as an open circuit without affecting the steady-state current.
132 Therefore, battery B_i in the RBS can be simplified as a series connection between a constant voltage
133 source u_i and a resistor r_i . Furthermore, the state of switch S_j in the RBS is represented by a binary
134 variable x_j , where 0 is ON and 1 is OFF. When the switch is closed, the circuit can be regarded as
135 a resistor with a very small resistance r_j . Finally, the external load is considered as a resistor with
136 resistance R_o .

137 For a given RBS structure, its directed graph model $G(V, E)$ is constructed as follows:

- 138 1. Nodes: The nodes in the directed graph correspond to the connection points of components in
139 the actual RBS. Assuming there are a total of N nodes in the RBS, for the sake of convenience,
140 the anode of the RBS is denoted as v_1 and the cathode as v_N .
- 141 2. Edges: The edges in the directed graph correspond to the batteries, switches, and external
142 electrical loads in the actual RBS. Therefore, there are three types of directed edges. For
143 battery B_i , its directed edge e_i is drawn from the cathode to the anode because the battery
144 in operation only allows current to flow in one direction. For switch S_j , since it is allowed to
145 work under bidirectional currents, it is represented by a pair of directed edges with two-way
146 directions. Regarding the external electronic load, because it is connected to the anode and
147 cathode of the RBS, a directed edge from v_N to v_1 represents it. In conclusion, for a given RBS
148 structure with N_b batteries and N_s switches, the number of directed edges is $N_b + 2N_s + 1$,
149 where 1 refers to the external electrical load.
- 150 3. Attributes of edges: Each edge is assigned two attributes, voltage difference and resistance,
151 based on the equivalent method mentioned above. The values for battery B_i , switch S_j , and
152 external loads correspond to (u_i, r_i) , $(0, r_j)$, and $(0, R_o)$, respectively.

153 2.2 Constraints and objective function

154 For a given RBS, determining its MAC involves maximizing the RBS output current while ensuring
155 that all battery currents do not exceed the batteries' MAC. This subsection establishes the con-
156 straints and objective function to determine the RBS's MAC through circuit analysis based on the
157 directed graph model provided in the previous section.

158 First, the topology in the directed graph model is represented in matrix form \mathbf{A} , known as the
159 incidence matrix and defined as follows:

$$a_{kl} = \begin{cases} 1, & \text{edge } l \text{ leaves node } k, \\ -1, & \text{edge } l \text{ enters node } k, \\ 0, & \text{otherwise.} \end{cases} \quad (1)$$

160 For a directed graph consisting of N nodes and $N_b + 2N_s + 1$ directed edges, its incidence matrix \mathbf{A}
 161 is an $N \times (N_b + 2N_s + 1)$ matrix. In this matrix, the rows and columns represent the nodes and edges
 162 of the directed graph, respectively. By distinguishing the components in the RBS corresponding to
 163 each column, \mathbf{A} can be rewritten as

$$\mathbf{A} = [\mathbf{A}_b \quad \mathbf{A}_s \quad \mathbf{A}_o], \quad (2)$$

164 where \mathbf{A}_b , \mathbf{A}_s , and \mathbf{A}_o are the submatrices corresponding to the batteries, switches, and external
 165 electrical load, respectively. To reduce the computational complexity, the dimensions of matrix \mathbf{A}
 166 are reduced. Since each directed edge has one node to leave and one to enter, the values in every
 167 column of \mathbf{A} sum to zero. Therefore, removing the last row will not result in a loss of information.
 168 Conversely, since each switch in the RBS is represented by a pair of directed edges with two-way
 169 directions, the two columns corresponding to the switch are mutually opposite. Thus, for the
 170 submatrix \mathbf{A}_s , only one column is retained for each pair of columns representing the same switch.
 171 As a result, \mathbf{A} can be reduced to an $(N - 1) \times (N_b + N_s + 1)$ matrix, denoted $\tilde{\mathbf{A}}$, for further calculation
 172 of current and voltage. Similar to Eq. (2), $\tilde{\mathbf{A}}$ can be rewritten as

$$\tilde{\mathbf{A}} = [\tilde{\mathbf{A}}_b \quad \tilde{\mathbf{A}}_s \quad \tilde{\mathbf{A}}_o]. \quad (3)$$

173 After obtaining the incidence matrix, the currents of all batteries and output in the RBS are
 174 determined by solving the circuit equations. According to Kirchhoff's laws, we have

$$\begin{cases} \tilde{\mathbf{A}}\mathbf{I} = \mathbf{0}, \\ \mathbf{U} = \tilde{\mathbf{A}}^T \mathbf{U}_n, \end{cases} \quad (4)$$

175 where \mathbf{I} and \mathbf{U} indicate the current and voltage difference arrays of the $N_b + N_s + 1$ edges, respectively,
 176 and \mathbf{U}_n is the voltage array of the $N - 1$ nodes. These directed edges are treated as generalized
 177 branches and expressed in matrix form as follows:

$$\mathbf{I} = \mathbf{Y}\mathbf{X}\mathbf{U} - \mathbf{Y}\mathbf{X}\mathbf{U}_s + \mathbf{I}_s, \quad (5)$$

178 where \mathbf{U}_s and \mathbf{I}_s denote the source voltage and source current of the generalized branches, respec-
 179 tively. Because all batteries have been equivalent to voltage sources rather than current sources in
 180 the previous subsection, all elements of the array \mathbf{I}_s are zero, whereas the elements of the array \mathbf{U}_s
 181 are equal to the first attribute of the corresponding edges in the directed graph. The matrix \mathbf{Y} in
 182 Eq. (5) is the admittance matrix of the circuit and is defined as the inverse of the impedance matrix.
 183 The elements on the diagonal of matrix \mathbf{Y} are equal to the reciprocal of the resistance, which is the
 184 second attribute of the corresponding edges in the directed graph. The off-diagonal elements of \mathbf{Y}
 185 are zero. \mathbf{X} is the state matrix that determines whether the RBS batteries and switches can pass

186 current. It is defined as

$$\mathbf{X} = \text{diag}(\underbrace{1, 0, \dots, 1}_{N_b \text{ of } 0/1}, \underbrace{1, 0, \dots, 1}_{N_s \text{ of } 0/1}, 1) = \begin{bmatrix} \mathbf{X}_b & & \\ & \mathbf{X}_s & \\ & & 1 \end{bmatrix}, \quad (6)$$

187 where element x_i of matrix \mathbf{X}_b indicates whether battery B_i has been removed from the circuit,
188 with $x_i = 1$ indicating removal and $x_i = 0$ indicating that battery B_i is still available to supply
189 power. When all batteries are healthy and capable of providing current to the external load, \mathbf{X}_b
190 is the identity matrix. The elements x_j of matrix \mathbf{X}_s determine whether switch S_j is closed, with
191 $x_j = 1$ indicating a closed switch and $x_j = 0$ indicating an open switch, which is consistent with the
192 previous subsection.

193 Theoretically, the output current I_o and the currents of each battery \mathbf{I}_b in the RBS can be
194 determined by solving Eqs. (4)–(6) under any given state \mathbf{X} . To further simplify the problem, it
195 is assumed that all batteries have the same electromotive force and internal resistance, which are
196 denoted u_b and r_b , respectively. This allows us to derive explicit expressions for I_o and \mathbf{I}_b . After
197 derivation and simplification, the output current I_o and the currents of each battery \mathbf{I}_b are ultimately
198 represented as Eqs. (7) and (8), respectively:

$$I_o = \frac{1}{R_o r_b} \tilde{\mathbf{A}}_o^T \mathbf{Y}_n^{-1}(\mathbf{X}) \tilde{\mathbf{A}}_b \mathbf{U}_b, \quad (7)$$

$$\mathbf{I}_b = \frac{1}{r_b^2} [\tilde{\mathbf{A}}_b^T \mathbf{Y}_n^{-1}(\mathbf{X}) \tilde{\mathbf{A}}_b \mathbf{U}_b - r_b \mathbf{U}_b], \quad (8)$$

200 where \mathbf{U}_b is an $N_b \times 1$ array with all elements equal to u_b , and \mathbf{Y}_n is the equivalent admittance
201 matrix of the circuit and is defined as

$$\mathbf{Y}_n(\mathbf{X}) = \frac{1}{R_o} \tilde{\mathbf{A}}_o \tilde{\mathbf{A}}_o^T + \frac{1}{r_b} \tilde{\mathbf{A}}_b \mathbf{X}_b \tilde{\mathbf{A}}_b^T + \frac{1}{r_s} \tilde{\mathbf{A}}_s \mathbf{X}_s \tilde{\mathbf{A}}_s^T. \quad (9)$$

202 To characterize the current output capacity of the RBS structure under different switching states,
203 an indicator η is defined by the ratio of I_o to $\max(\mathbf{I}_b)$:

$$\eta = \frac{I_o}{\max(\mathbf{I}_b)}. \quad (10)$$

204 Finally the problem of finding the MAC can be formulated as

$$\max \eta(\mathbf{X}_s) \quad (11)$$

$$\text{s.t. } \max(\mathbf{I}_b) \leq I_m, \quad (12)$$

205 where I_m is the MAC of the battery.

206 However, it remains computationally difficult to solve Eq. (11) because of \mathbf{Y}_n^{-1} . On one hand,
207 the introduction of nonlinear terms by \mathbf{Y}_n^{-1} renders many methods in linear optimization unsuitable
208 for this problem. On the other hand, the rank of \mathbf{Y}_n is proportional to the number of batteries and

209 switches, which can be very large for a large RBS, leading to a significant computational burden.
 210 As a result, intelligent algorithms that rely on evolution by iteration may face efficiency problems
 211 when dealing with a large RBS. To address this issue, the problem should be considered from the
 212 perspective of guiding the RBS to reconstruct as many parallel structures as possible. Consequently,
 213 a greedy algorithm based on the shortest path is proposed. The detailed implementation of this
 214 algorithm is presented in the following two subsections.

215 **2.3 Shortest path**

216 The path p used in this method is defined as the complete route that passes through one battery (or a
 217 consecutive series of batteries) and closed switches, connecting the anode v_1 to the cathode v_N of the
 218 RBS. By applying a penalty to the series-connected batteries on the path, where additional batteries
 219 imply a greater distance, the algorithm encourages the RBS to form parallel structures to the extent
 220 possible. In addition, to reduce the number of switches controlled during the reconstruction process,
 221 a penalty is also applied to the total number of switches on the path while ensuring the minimum
 222 number of batteries. Therefore, the distance ω of path p is

$$\omega(p) = N_s n_b(p) + n_s(p), \quad (13)$$

223 where N_s is the total number of switches in the system, and $n_b(p)$ and $n_s(p)$ are number of batteries
 224 and switches in path p , respectively. Moreover, the shortest path SP_i is defined as the path with
 225 the minimum ω for battery B_i :

$$SP_i = \arg \min_{p \in P_i} \omega(p), \quad (14)$$

226 where P_i is the set of all paths from v_1 to v_N that pass through directed edge i .

227 SP_i can be solved by the Dijkstra algorithm. The Dijkstra algorithm is a graph-search method
 228 that finds the shortest path between two given nodes in a weighted graph, efficiently solving the
 229 single-source shortest-path problem. Denoting the cathode and anode of battery B_i as v_i^- and v_i^+
 230 respectively, then path p of battery B_i can be divided into three segments: $v_1 \rightarrow v_i^-$, $v_i^+ \rightarrow v_N$, and
 231 $v_i^- \rightarrow v_i^+$. $v_i^- \rightarrow v_i^+$ is the directed edge corresponding to battery B_i . With the Dijkstra algorithm,
 232 shortest paths for $v_1 \rightarrow v_i^-$ and $v_i^+ \rightarrow v_N$ can be calculated under the weights given in Eq. (13) and
 233 denoted $SP(v_i^- \rightarrow v_i^+)$ and $SP(v_i^+ \rightarrow v_N)$, respectively. Finally, SP_i for battery B_i is formed by
 234 the complete path, which consists of $SP(v_1 \rightarrow v_i^-)$, $v_i^- \rightarrow v_i^+$, and $SP(v_i^+ \rightarrow v_N)$.

235 **2.4 Greedy algorithm**

236 From the perspective of series vs parallel connections, integrating more batteries into the circuit
 237 through their shortest paths (SPs) results in more batteries connected in parallel, thereby increasing
 238 the total output current of the RBS. However, conflicts may arise between the SPs of different
 239 batteries. For instance, the SPs of two batteries might form a short-circuit RBS structure, which is
 240 not allowed. To address this issue, a greedy algorithm incorporates as many SPs as possible while
 241 satisfying the reconstruction requirements.

242 The algorithm (see pseudo-code in Algorithm 1) is illustrated in Fig. 4 and is summarized as
 243 follows: First, the SPs are obtained by using Eqs. (13) and (14) in conjunction with the Dijkstra
 244 search. Next, the matrix \mathbf{A} is calculated using Eq. (1), and the initial N_{set} is set to N_b . The
 245 algorithm uses a dichotomy method to iteratively check until convergence different combinations of
 246 c_b batteries from N_b and updates N_{set} . For each combination, the algorithm constructs an effective
 247 solution if possible and calculates the currents I_o and \mathbf{I}_b by using Eqs. (7) and (8). If the maximum
 248 current \mathbf{I}_b is less than or equal to I_m , η is calculated by using Eq. (10), and the maximum η is
 249 updated accordingly. Finally, the algorithm outputs the maximum η once N_{set} converges.

250 3 Case Study

251 3.1 Structures

252 Currently, two types of RBS structures have been proposed by Visairo et al. [11] and Lawson et
 253 al. [15], both of which have seen real use. The primary goal of Visairo's structure (Fig. 5b) is
 254 to dynamically adjust the RBS output power. However, the isolation of unhealthy batteries is not
 255 sufficiently addressed in their work. Lawson et al. designed the RBS structure shown in Fig. 5a
 256 to isolate batteries. Although this structure easily isolates batteries, it cannot dynamically adjust
 257 the output current of the RBS. Based on the structures of Visairo and Lawson, this paper proposes
 258 the structure shown in Fig. 5c. By integrating the Visairo RBS structure into the Lawson RBS
 259 structure, the proposed structure not only has the flexibility to switch the batteries between series,
 260 parallel, and mixed series-parallel modes but also allows the isolation of highly degraded batteries
 261 from the RBS. These four-battery RBS structures are investigated in the case study, including the
 262 scenarios with random isolated batteries.

263 3.2 Result

264 As shown in Fig. 5c, the new RBS structure consists of four batteries and 19 switches. Figure 6a
 265 shows the corresponding directed graph, which is composed of 18 nodes and 43 edges. Batteries B_1 ,
 266 B_2 , B_3 , and B_4 are denoted by green directed edges in the graph, and the 19 switches are represented
 267 by gray directed edges with bidirectional arrows. The external electrical load is treated as a directed
 268 edge from the cathode of the RBS (i.e., node 18) to the anode (i.e., node 1), as indicated by the
 269 blue directed edge in the graph. Using Eq. (13) and the Dijkstra algorithm, the SPs of the four
 270 batteries in the RBS structure of Fig. 5c are highlighted in red in Figs. 6b and 6e. Finally, the
 271 calculated MACs of the structure in Fig. 5c are listed in Tab. 1 and shown in Fig. 6f, as obtained
 272 by the greedy algorithm 1. Tab. 1 contains the states of the switches, the output current I_o , the
 273 battery current \mathbf{I}_b , and the ratio η of the RBS structure with all batteries in good health when the
 274 RBS output reaches the MAC. Fig. 6f presents the corresponding circuit, with the red highlight
 275 indicating that the current is flowing through the respective branches.

276 Similarly, the results of the MAC calculation for the structures in Figs. 5a and 5b are listed in
 277 Tabs. 2 and 3, respectively.

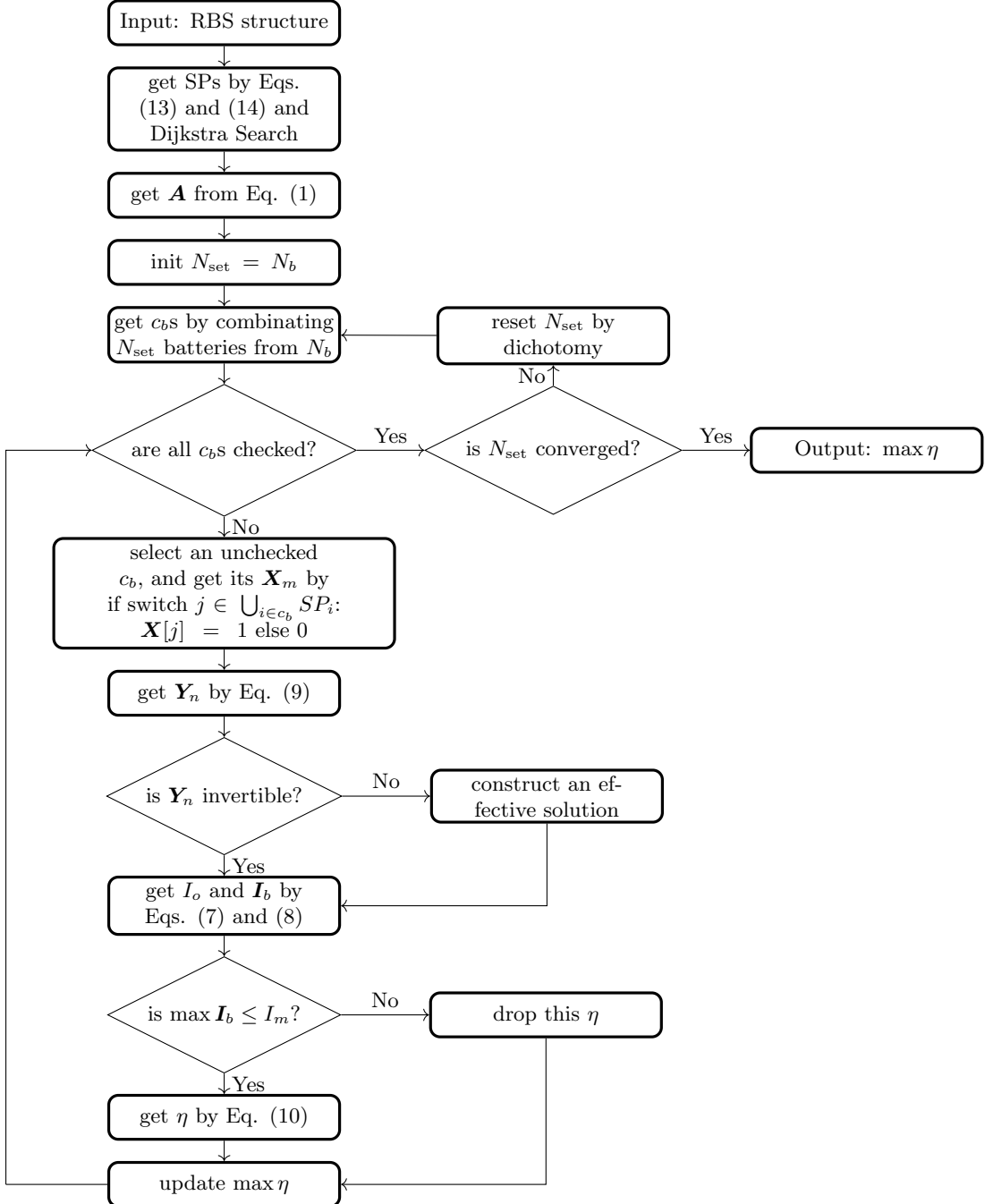


Figure 4: The computational flowchart of the MAC for a given RBS.

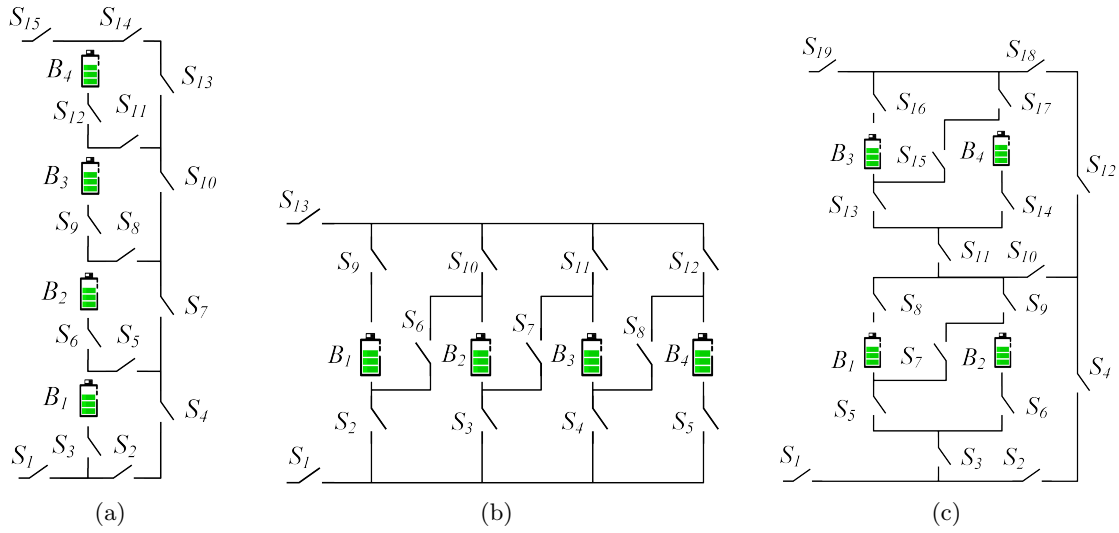


Figure 5: The four-battery RBS structures proposed by (a) Lawson [15], (b) Visairo [11], and (c) this paper.

Table 1: Calculated MAC for four-battery RBS structure in Fig. 5c.

Structure	Figure 5c with four batteries and 19 switches
Switch on	$S_1, S_3, S_5, S_6, S_8, S_9, S_{10}, S_{12}, S_{18}, S_{19}$
I_o	$2u_b/(2R_o + r_b)$
I_b	$[u_b/(2R_o + r_b), u_b/(2R_o + r_b), 0, 0]$
$\max \eta$	2

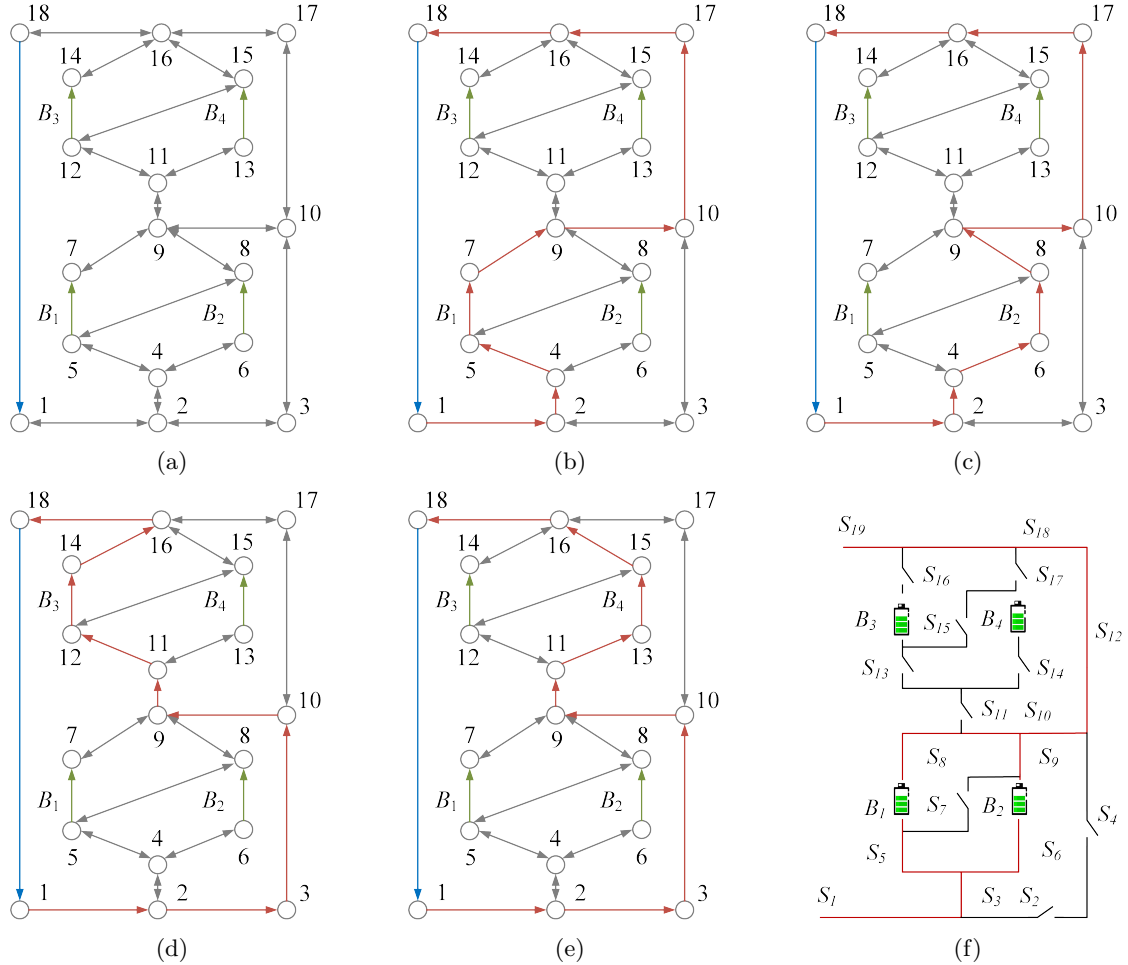


Figure 6: For the RBS structure in Fig. 5c, (a) its directed graph and the SPs (highlighted in red) of battery (b) B_1 , (c) B_2 , (d) B_3 , and (e) B_4 . (f) Circuit of RBS with its output reaching the MAC.

278 To verify and compare the results from the greedy algorithm, we also used a brute-force algorithm
 279 that iterates through all possible switch states to calculate the MAC of the same three RBSs. The
 280 final results are the same as the results shown in Tabs. 1–3. The method uses the greedy algorithm
 281 to calculate 11, 11, and 1 reconfigured structures for the RBS structure in Figs. 5c, 5a, and 5b,
 282 respectively. For the same RBS, the method counts all possible switch states, which equates to 2^{19} ,
 283 2^{15} , and 2^{13} structures, respectively.

Table 2: MAC Calculating result of the four-battery RBS structure in Fig. 5a.

Structure	Figure 5a with 4 batteries and 15 switches
Switch ON	$S_1, S_3, S_5, S_7, S_{10}, S_{13}, S_{14}, S_{15}$
I_o	$u_b/(R_o + r_b)$
I_b	$[u_b/(R_o + r_b), 0, 0, 0]$
$\max \eta$	1

Table 3: MAC Calculating result of the four-battery RBS structure in Fig. 5b.

Structure	Figure 5b with 4 batteries and 13 switches
Switch ON	$S_1, S_2, S_3, S_4, S_5, S_9, S_{10}, S_{11}, S_{12}, S_{13}$
I_o	$4u_b/(4R_o + r_b)$
I_b	$[u_b/(4R_o + r_b), u_b/(4R_o + r_b), u_b/(4R_o + r_b), u_b/(4R_o + r_b)]$
$\max \eta$	4

284 Furthermore, the RBS with isolated batteries is taken into consideration and calculated. The
 285 MAC calculation results for the three structures under study, with varying numbers of isolated
 286 batteries, are presented in Tab. 4. Figs. 7a–7d illustrate the corresponding switch-control schemes
 287 for the new structure proposed in this paper under different conditions of isolated batteries.

Table 4: Variation of MAC with the number of isolated batteries for different RBS structures, including the structure proposed by Lawson et al., Visairo et al., and the structure proposed in this paper.

Number of isolated batteries	η of RBS structure		
	This paper	Visairo	Lawson
0	2	4	1
1	2	3	1
2	2 ^a or 1 ^b	2	1
3	1	1	1

^a Isolate two batteries within the same substructure, as shown in Fig. 7b.

^b Isolate one battery in each of the two substructures, as shown in Fig. 7c.

3.3 Discussion

288 Consider first the results shown in Fig. 6f and listed in Tab. 1. When B_1 and B_2 or B_3 and B_4
 289 are connected in parallel, the RBS outputs the maximum current, which is $\eta = 2$ (i.e., twice the

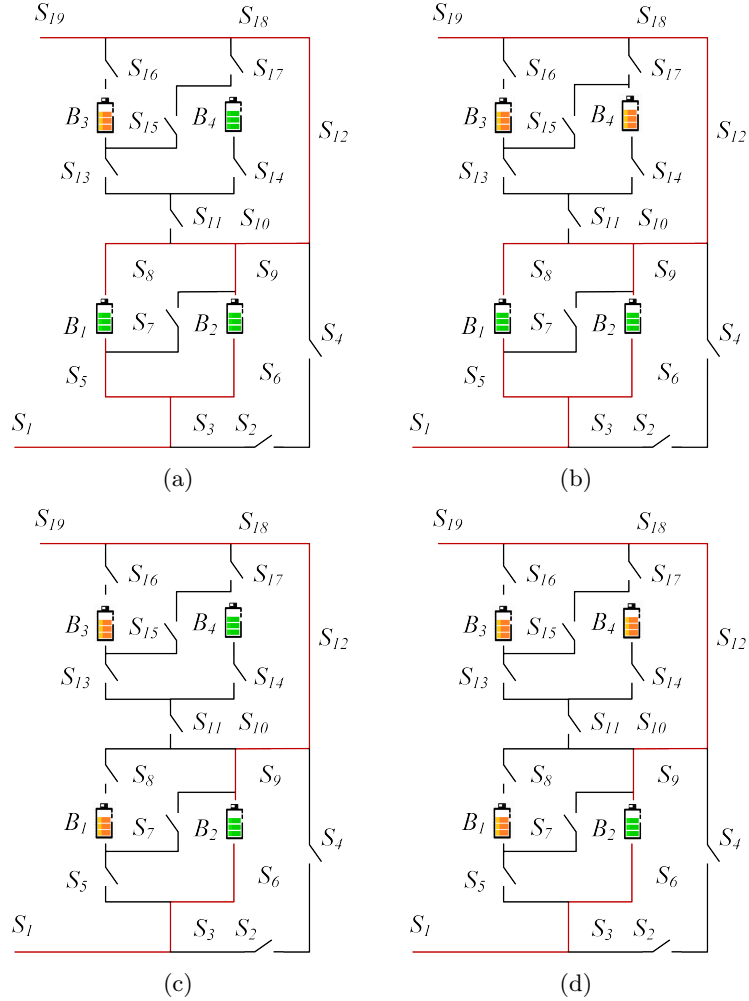


Figure 7: Circuit states of MACs when isolating (a) one, (b) two (best case), (c) two (worst case), and (d) three batteries for the structure in Fig. 5c.

291 current output of a single battery in the RBS). Adding more batteries to the main circuit only forms
 292 a series structure and does not improve the MAC. Therefore, the state of the switches given in Tab.
 293 1 maximizes the RBS output current. The brute-force method, which go through all possible switch
 294 states, also gives the same result.

295 The literature contains no report on an algorithm for calculating the MAC of an RBS. The
 296 brute-force algorithm, which goes through all possible switch states, is the most straightforward way
 297 to determine the MAC and is used as a benchmark for the proposed greedy algorithm. If an RBS
 298 has N_b batteries and N_s switches and the corresponding directed graph has N nodes, 2^{N_s} iterations
 299 are required to traverse all reconfigured structures. Calculating each reconfigured structure using
 300 Eqs. (7)–(10) requires matrix inversion and matrix multiplication, which has a time complexity
 301 of $O(N^3 + 2N^2N_b + N^2N_s + NN_b^2)$. Therefore, the time complexity of the brute-force algorithm
 302 is $O((N^3 + 2N^2N_b + N^2N_s + NN_b^2)2^{N_s})$. The greedy algorithm proposed in this paper requires
 303 that SP be found for each battery, which requires N_b iterations. Each SP can be obtained by
 304 several applications of Dijkstra's algorithms. Therefore, the total time complexity for calculating
 305 all SPs is $O(N_b(N_b + 2N_s)\log_{10}N)$. According to Appendix 1, the RBS can reconfigure $C_{N_b}^{N_{\text{set}}}$
 306 structures by selecting N_{set} batteries from N_b batteries, which gives $\sum_{N_{\text{set}}=1}^{N_b} C_{N_b}^{N_{\text{set}}} / N_b \approx 2^{N_b} N_b^{-1}$
 307 on average. Thus, with the bisection method, the time complexity of the greedy algorithm is
 308 $O((N^3 + 2N^2N_b + N^2N_s + NN_b^2)2^{N_b} N_b^{-1} \log_{10} N_b + N_b(N_b + 2N_s)\log_{10} N)$. Based on currently
 309 proposed RBS structures [23, 24, 25, 26, 27, 28], the number N_b of batteries, N_s of switches, and
 310 N of nodes are quantitatively related as follows: $N_s \approx (3-5)N_b$, $N \approx N_s$. After simplifying, the
 311 time complexity of the method with greedy algorithm is $O(2^{N_b} N_s^2 \log_{10} N_b)$, while it is $O(2^{N_s} N_s^3)$
 312 for the method with brute force algorithm. Therefore, as the RBS grows, especially in the number of
 313 switches, the greedy algorithm gains an advantage over the brute-force algorithm. This is confirmed
 314 by the number of structures required to determine the MAC in the previous section. Compared with
 315 the brute-force algorithm, the method based on the greedy algorithm is 3 000 to 48 000 times more
 316 efficient, which is theoretically $N_s 2^{N_s - N_b} \log_{10} N_b$ times according to the above time-complexity
 317 analysis. This benefits from two key points:

- 318 (1) The SPs guide the RBS to reconfigure reasonable structures rather than blindly going through
 319 all possible structures. This reduces the complexity from 2^{N_s} to 2^{N_b} , which is the main reason
 320 for the improvement in efficiency.
- 321 (2) The bisection method further accelerates this process, reducing the complexity from 2^{N_b} to
 322 $2^{N_b} N_B^{-1} \log_{10} N_b$.

323 However, the greedy algorithm proposed in this paper still contains exponential terms in the time
 324 complexity, which means it may not be able to handle extremely large RBS structures having large
 325 N_b .

326 Note that η is used as the objective function instead of I_o in solving for the MAC. This choice
 327 makes the resulting MAC more reasonable. As shown in Tab. 1, I_o and I_b are functions of R_o ,
 328 u_b , and r_b . However, when I_o is used as the objective function, even for the same RBS structure,
 329 the MAC solution and corresponding switch states could change due to different external electrical
 330 appliances. This would increase the difficulty and uncertainty of designing the RBS structure. To

331 eliminate this problem, the ratio $\eta = I_o / \max \mathbf{I}_b$ is adopted as the objective function in our research.
332 Recall that η reflects only the structure's ability to output current, rather than the actual current
333 outputting by the battery system. Assuming that the MAC of batteries in the RBS is I_m , the
334 maximum output current of the RBS structure can be calculated as ηI_m by determining the value
335 of η for the structure.

336 The method proposed in this paper facilitates the design of RBSs in the following ways: Most
337 currently proposed RBS structures [23, 24, 25, 26, 27, 28] have simple topological characteristics, so
338 calculating the MACs is relatively straightforward, even intuitive. However, these simple structures
339 do not always fully satisfy the requirements of complex applications, such as dynamically adapting
340 the circuit to variable and random operating conditions or actively equalizing differences between
341 batteries in the RBS. Moreover, isolating the batteries disrupts the original regularity and symmetry
342 of the topology, which complicates the otherwise simple structure, and the maximum output current
343 of the system becomes more challenging to obtain. In contrast, the proposed method calculates the
344 MAC of arbitrary RBS structures, notably the complex and flexible RBS structures.

345 To illustrate this point, the MACs of three RBS structures mentioned above are calculated after
346 isolating one or more of the batteries, as shown in Tab. 4. Specifically, for the structure presented
347 in Fig. 5c, the corresponding circuit states for the MACs when isolating one to three batteries are
348 depicted in Figs. 7a–7d. This structure has two cases in which two batteries are isolated: one is
349 to isolate two batteries within the same substructure (Fig. 7b), in which case $\eta = 2$; the other
350 is to isolate one battery in each of the two substructures (Fig. 7c), in which case $\eta = 1$. The
351 results in Figs. 7a–7d show that the proposed method provides reasonable outcomes for isolating
352 any number of batteries in any position. Furthermore, the output current for the three RBSs with
353 isolated batteries is also shown in Tab. 4. For the structure proposed by Lawson et al., the MAC is
354 independent of the number of isolated batteries. However, for Visairo's structure, the MAC decreases
355 upon increasing the number of isolated batteries. Nevertheless, the MAC of the structure proposed
356 in this work falls between the MACs of these two structures. This result indicates that the structure
357 proposed in this paper has a larger MAC than Lawson's for the same number of batteries and has
358 a wider range of regulation of the output current.

359 4 Conclusion

360 This paper proposes a pervasive and automated method to efficiently compute the MAC of an
361 RBS. The method is implemented by a greedy algorithm combined with an improved directed graph
362 model. Not only does the method provides the same global MAC calculation results as the brute
363 force method, but it also improves the calculation efficiency by 3 000 to 48 000 times for three RBS
364 structures in the case study. Theoretically, for an RBS with N_s switches and N_b batteries, the
365 efficiency of the proposed method is $N_s 2^{N_s - N_b} \log_{10} N_b$ times that of the brute-force method, which
366 is mainly because of using the batteries' SPs to guide the RBS to reconfigure reasonable structures
367 rather than blindly going through all possible structures. The main advantage of this method is
368 its ability to calculate the MAC of RBSs with arbitrary structures. Even in scenarios with random
369 isolated batteries, the proposed method remains effective. This method helps to fully tap the current

³⁷⁰ output potential of the RBS, guide the RBS structure design and optimization in the design stage,
³⁷¹ and assist in evaluating the current-overload risk of the system in practical applications.

³⁷² 5 Appendix

Algorithm 1: Get the max available currents of a certain RBS

Data: Directed graph model $G(V, E)$ of the RBS
Result: $\max \eta$

```
1 for  $i \in E_b$  do
2    $P_i \leftarrow \{path|starts at v_1 and ends at v_n\};$ 
3    $SP_i \leftarrow p_i$  which has the minimum  $\omega(p_i)$  among all  $p_i \in P_i.$ 
4 end
5 get  $A$  by Eq. 1;
6 while not yet determine  $\max \eta$  do
7    $N_{set} \leftarrow$  number of selected SPs calculated by dichotomy;
8    $C_b \leftarrow$  set of all combinations of  $N_{set}$  batteries from  $N_b;$ 
9   for  $c_b \in C_b$  do
10     $x_s \leftarrow$  list of all switches' state:  $x_s[j] = 1$  if  $j \in \bigcup_{i \in c_b} SP_i$  else 0;
11     $X \leftarrow diag[1, 1, \dots, 1, x_s];$ 
12    get  $Y_n$  by Eq. 9;
13    if  $Y_n$  is invertible then
14      pass
15    else
16      construct an effective solution
17    end
18    get  $I_o$  by Eq. 7;
19    get  $I_b$  by Eq. 8;
20    if  $\max(I_b) \leq I_m$  then
21       $\eta \leftarrow I_o / \max(I_b);$ 
22    else
23      break
24    end
25  end
26 end
```

³⁷³ Acknowledgments

³⁷⁴ Author Contributions

³⁷⁵ B. Xu conceived the main idea, formulated the overarching research goals and aims, designed the
³⁷⁶ algorithm, and reviewed and revised the manuscript. G. Hua developed and analyzed the model,
³⁷⁷ implemented the code and supporting algorithms, and wrote the initial draft. C. Qian provided
³⁷⁸ critical review, commentary, and revisions. Q. Xia contributed to shaping the research, analysis,
³⁷⁹ and manuscript. B. Sun conducted the research and investigation process. Y. Ren secured the

380 funding and supervised the project. Z. Wang verified the results and provided necessary resources.

381 **Funding**

382 This work was supported by the National Natural Science Foundation of China (NSFC, No.52075028).

383 **Conflicts of Interest**

384 The authors declare that there is no conflict of interest regarding the publication of this article.

385 **Data Availability**

386 This work does not require any data to be declared or publicly disclosed.

387 **References**

- 388 [1] Yuqing Yang, Stephen Bremner, Chris Menictas, and Merlinde Kay. Battery energy storage
389 system size determination in renewable energy systems: A review. *Renewable and Sustainable
390 Energy Reviews*, 91:109–125, August 2018.
- 391 [2] Luanna Maria Silva de Siqueira and Wei Peng. Control strategy to smooth wind power output
392 using battery energy storage system: A review. *Journal of Energy Storage*, 35:102252, March
393 2021.
- 394 [3] Eugene Schwanbeck and Penni Dalton. International Space Station Lithium-ion Batteries for
395 Primary Electric Power System. In *2019 European Space Power Conference (ESPC)*, pages 1–1.
396 IEEE, September 2019.
- 397 [4] Lihua Zhang. Development and Prospect of Chinese Lunar Relay Communication Satellite.
398 *Space: Science & Technology*, 2021, January 2021.
- 399 [5] Jaephil Cho, Sookkyung Jeong, and Youngsik Kim. Commercial and research battery technologies
400 for electrical energy storage applications. *Progress in Energy and Combustion Science*,
401 48:84–101, June 2015.
- 402 [6] Naixing Yang, Xiongwen Zhang, BinBin Shang, and Guojun Li. Unbalanced discharging and
403 aging due to temperature differences among the cells in a lithium-ion battery pack with parallel
404 combination. *Journal of Power Sources*, 306:733–741, February 2016.
- 405 [7] Fei Feng, Xiaosong Hu, Lin Hu, Fengling Hu, Yang Li, and Lei Zhang. Propagation mechanisms
406 and diagnosis of parameter inconsistency within Li-Ion battery packs. *Renewable and Sustainable
407 Energy Reviews*, 112:102–113, September 2019.
- 408 [8] J. A. Jeevarajan and C. Winchester. Battery Safety Qualifications for Human Ratings. *Interface
409 magazine*, 21(2):51–55, January 2012.

- 410 [9] Daniel Vázquez Pombo. A Hybrid Power System for a Permanent Colony on Mars. *Space: Science & Technology*, 2021, January 2021.
- 411
- 412 [10] Weiji Han, Torsten Wik, Anton Kersten, Guangzhong Dong, and Changfu Zou. Next-Generation Battery Management Systems: Dynamic Reconfiguration. *IEEE Industrial Electronics Magazine*, 14(4):20–31, December 2020.
- 413
- 414
- 415 [11] H. Visairo and P. Kumar. A reconfigurable battery pack for improving power conversion efficiency in portable devices. In *2008 7th International Caribbean Conference on Devices, Circuits and Systems*, pages 1–6. IEEE, April 2008.
- 416
- 417
- 418 [12] Song Ci, Jiucai Zhang, Hamid Sharif, and Mahmoud Alahmad. A novel design of adaptive reconfigurable multicell battery for power-aware embedded networked sensing systems. In *IEEE GLOBECOM 2007-IEEE Global Telecommunications Conference*, pages 1043–1047. IEEE, 2007.
- 419
- 420
- 421
- 422 [13] Jan Engelhardt, Tatiana Gabderakhmanova, Gunnar Rohde, and Mattia Marinelli. Reconfigurable stationary battery with adaptive cell switching for electric vehicle fast-charging. In *2020 55th International Universities Power Engineering Conference (UPEC)*, pages 1–6, 2020.
- 423
- 424
- 425 [14] Jan Engelhardt, Jan Martin Zepter, Tatiana Gabderakhmanova, Gunnar Rohde, and Mattia Marinelli. Double-string battery system with reconfigurable cell topology operated as a fast charging station for electric vehicles. *Energies*, 14(9):2414, 2021.
- 426
- 427
- 428 [15] Barrie Lawson. A Software Configurable Battery. *EVS26 International Battery, Hybrid and Fuel Cell Electric Vehicle Symposium*, 2012.
- 429
- 430 [16] Liang He, Linghe Kong, Siyu Lin, Shaodong Ying, Yu Gu, Tian He, and Cong Liu. Reconfiguration-assisted charging in large-scale lithium-ion battery systems. In *2014 ACM/IEEE International Conference on Cyber-Physical Systems (ICCPs)*, pages 60–71. IEEE, 2014.
- 431
- 432
- 433
- 434 [17] Hahnsang Kim and Kang G Shin. On dynamic reconfiguration of a large-scale battery system. In *2009 15th IEEE Real-Time and Embedded Technology and Applications Symposium*, pages 87–96. IEEE, 2009.
- 435
- 436
- 437 [18] Weiji Han, Anton Kersten, Changfu Zou, Torsten Wik, Xiaoliang Huang, and Guangzhong Dong. Analysis and estimation of the maximum switch current during battery system reconfiguration. *IEEE Transactions on Industrial Electronics*, 69(6):5931–5941, 2021.
- 438
- 439
- 440 [19] Si-Zhe Chen, Yule Wang, Guidong Zhang, Le Chang, and Yun Zhang. Sneak Circuit Theory Based Approach to Avoiding Short-Circuit Paths in Reconfigurable Battery Systems. *IEEE Transactions on Industrial Electronics*, 68(12):12353–12363, 2021.
- 441
- 442
- 443 [20] Liang He, Lipeng Gu, Linghe Kong, Yu Gu, Cong Liu, and Tian He. Exploring Adaptive Reconfiguration to Optimize Energy Efficiency in Large-Scale Battery Systems. In *2013 IEEE 34th Real-Time Systems Symposium*, pages 118–127, December 2013.
- 444
- 445

- 446 [21] Hongwen He, Rui Xiong, Xiaowei Zhang, Fengchun Sun, and JinXin Fan. State-of-Charge
447 Estimation of the Lithium-Ion Battery Using an Adaptive Extended Kalman Filter Based on
448 an Improved Thevenin Model. *IEEE Transactions on Vehicular Technology*, 60(4):1461–1469,
449 May 2011.
- 450 [22] S.M. Mousavi G. and M. Nikdel. Various battery models for various simulation studies and
451 applications. *Renewable and Sustainable Energy Reviews*, 32:477–485, April 2014.
- 452 [23] Song Ci, Jiucai Zhang, Hamid Sharif, and Mahmoud Alahmad. A Novel Design of Adaptive
453 Reconfigurable Multicell Battery for Power-Aware Embedded Networked Sensing Systems. In
454 *IEEE GLOBECOM 2007-2007 IEEE Global Telecommunications Conference*, pages 1043–1047,
455 November 2007.
- 456 [24] Mahmoud Alahmad, Herb Hess, Mohammad Mojarradi, William West, and Jay Whitacre. Bat-
457 tery switch array system with application for JPL’s rechargeable micro-scale batteries. *Journal*
458 *of Power Sources*, 177(2):566–578, March 2008.
- 459 [25] Hahnsang Kim and Kang G. Shin. Dependable, efficient, scalable architecture for manage-
460 ment of large-scale batteries. In *Proceedings of the 1st ACM/IEEE International Conference*
461 *on Cyber-Physical Systems*, ICCPS ’10, pages 178–187, New York, NY, USA, April 2010. As-
462 sociation for Computing Machinery.
- 463 [26] Younghyun Kim, Sangyoung Park, Yanzhi Wang, Qing Xie, Naehyuck Chang, Massimo Pon-
464 cino, and Massoud Pedram. Balanced reconfiguration of storage banks in a hybrid electrical
465 energy storage system. In *2011 IEEE/ACM International Conference on Computer-Aided De-*
466 *sign (ICCAD)*, pages 624–631, November 2011.
- 467 [27] Taesic Kim, Wei Qiao, and Liyan Qu. A series-connected self-reconfigurable multicell battery
468 capable of safe and effective charging/discharging and balancing operations. In *2012 Twenty-*
469 *Seventh Annual IEEE Applied Power Electronics Conference and Exposition (APEC)*, pages
470 2259–2264, February 2012.
- 471 [28] Liang He, Linghe Kong, Siyu Lin, Shaodong Ying, Yu Gu, Tian He, and Cong Liu.
472 Reconfiguration-assisted charging in large-scale Lithium-ion battery systems. In *2014*
473 *ACM/IEEE International Conference on Cyber-Physical Systems (ICCPs)*, pages 60–71, April
474 2014.

